

On using mCherry as a label for use in wide-field homo-FRET induced fluorescence anisotropy microscopy

Kiefer van Teutem
Studentnummer 3760456
Utrecht University

January 2014

Abstract

Förster Resonance Energy Transfer (FRET) can be used to determine the interactions between proteins in cells. When using identical donor and acceptor molecules, it is referred to as homo-FRET. In this thesis we explore the possibilities of homo-FRET induced fluorescence anisotropy microscopy, and in particular we compare mCherry and GFP as labeling proteins. We found that the effect of cell autofluorescence on the accuracy of our measurements was greatly reduced by measuring in the red part of the spectrum (using mCherry). We expect to be able to measure the anisotropy of mCherry in cells with an accuracy of about 0.002, although more experiments are necessary to confirm this. Furthermore this thesis serves as a simple guide to homo-FRET and fluorescence anisotropy microscopy, and includes an extensive measurement and data analysis protocol.

Contents

0	Introduction	1
1	Relevance	1
2	Theory	2
2.1	Fluorescence	2
2.2	FRET	2
2.3	Anisotropy	3
2.4	Polarization affecting factors	8
2.5	Protein clustering	9
2.6	Measuring anisotropy: T-setup vs. L-setup, Steady-state vs. Time-resolved, Wide-field vs. Confocal	9
2.7	Some numbers	10
3	Experimental setup	12
3.1	The dichroic cubes	13
3.2	The cameras	14
3.3	Alignment	14
3.4	Consequences of the setup	15
3.5	Autofluorescence	18
4	The measurement process	20
4.1	Image beads	20
4.2	Image rhodamine	20
4.3	Image mCherry	20
4.4	Image unlabeled cells	21
4.5	Image labeled cells of interest	21
5	Data analysis	22
5.1	Determining T	22
5.2	Determining G	22
5.3	Determining the maximum anisotropy	23
5.4	Determining the autofluorescence	23
5.5	Determining the anisotropies	23
5.6	Saving the data	24
6	Uncertainty	26
6.1	Photon statistics uncertainty	26
7	Reference measurements	27
7.1	Background	27
7.2	Photon statistics	27
7.3	Comparison of rolling and global measurement	27

7.4	Explanation for all camera abberations	28
7.5	Intensity comparison of dichroic cubes A, B and C	29
7.6	Factors in the environmental background	29
7.7	Intensity comparison of Rhodamine-B, Fluorescein, mCherry and GFP	30
7.8	Camera alignment with different dichroic cubes	30
7.9	G-factor measurements with dichroic B	30
7.10	G-factor measurements with dichroic C	31
7.11	The anisotropy of mCherry in glycerol	32
7.12	Autofluorescence with dichroics A and C	33
7.13	Re-evaluation of uncertainties	33
8	Conclusions	34
9	Discussion	34
10	MATLAB Scripts	37

0 Introduction

By measuring the rate of FRET (Förster Resonance Energy Transfer) in a sample, it is possible to determine the interactions between fluorescent molecules such as fluorescent proteins. Generally this is done using a donor molecule and a different acceptor molecule. The rate of FRET is then determined by either FLIM (fluorescence lifetime imaging) or by measuring the (long time) fluorescence intensity of the acceptor-molecule. This is referred to as "hetero-FRET". However, it is also possible to measure FRET between identical molecules. This is called homo-FRET and it has some distinct advantages over hetero-FRET, which we will discuss later. In this thesis I describe a method for measuring homo-FRET. This is a continuation of the work of Nivard Kagie [1], whose setup I'll be using. The goal of this research is to try to improve the method, and in particular to investigate the benefits of using mCherry instead of GFP as the labeling molecule. Unfortunately I was unable to perform the final measurements, with actual mCherry labeled cells. However, I was able to improve the setup and workflow and make a comparison between using mCherry and GFP as a labeling protein. This thesis should therefore be seen as a guide to using homo-FRET microscopy, and as a guide for future research with mCherry as a homo-FRET labeling protein.

1 Relevance

Being able to quickly and relatively cheaply measure the clustering of proteins in cells can be of great value to biological research. Take for example the epidermal growth factor receptor (EGFR), which is a receptor protein found on the membranes of cells. When exposed to EGF (Epidermal Growth Factor) it gets activated and starts a series of reactions which promotes DNA synthesis and cell proliferation. Overexpression of EGFR can lead to uncontrollable cell-division, which can cause cancer. Since the clustering of the EGFR protein on the membrane influences its activity, being able to measure protein clustering could aid in cancer research. Protein clustering occurs on too small a scale to be directly observed through regular light microscopy. Using electron microscopy is possible but time consuming, expensive, and the sample preparation is complicated. Being able to determine protein clustering using a regular microscope would therefore be a great alternative.

2 Theory

2.1 Fluorescence

Fluorescence is the process whereby an atom or molecule (a fluorophore) emits a photon after being excited by another photon. When the excitation photon is absorbed, this energy is used to get one of the electrons into a different quantum-state with a higher energy. The ground state is called S0 and the first excited state S1. Because of fine-structure splitting each of these states is split up into a number of different states, each of which has a slightly different energy. A typical fluorescence process is depicted in the Jablonski-diagram below (figure 1). When the molecule absorbs the excitation photon, its state changes to one of the higher splittings of the S1 state. The electron quickly (on the order of 10^{-22} seconds) drops into the regular S1 state through non-radiative processes. After some time (on the order of nanoseconds), the electron decays to one of the splittings of the ground state, while emitting a photon. Finally the electron loses its last bit of extra energy by decaying to the ground state, again through a quick, non-radiative process (10^{-22} seconds). Since the wavelength of a photon is inversely proportional to the energy difference in the decay process, we can now see why typically the emitted photon has a longer wavelength than the original photon. It is possible for the emitted photon to have a shorter wavelength in the case of two-photon excitation, but we will not get into that in this thesis. The rate at which an excited molecule emits a photon, is called the radiative decay rate $k_r = \frac{1}{\tau_r}$ where τ_r is the average radiative lifetime. It is also possible that the decay is purely non-radiative, and all the energy is converted into kinetic energy/heat. The rate at which this occurs is called the non-radiative decay rate $k_{nr} = \frac{1}{\tau_{nr}}$. Clearly the total decay rate k is $k_r + k_{nr}$. The quantum yield (QY) Φ of a fluorescent molecule is defined as the ratio between the radiative and the total decay rate:

$$\Phi = \frac{k_r}{k_r + k_{nr}} = \frac{\tau_{nr}}{\tau_r + \tau_{nr}} \quad (1)$$

The probability that a fluorophore is still excited at a time t after excitation is $e^{-(k_r+k_{nr})t}$, so the expected emission rate after a time t is $k_r e^{-(k_r+k_{nr})t}$. The total amount of radiative emission from a single excitation is:

$$\int_0^\infty k_r e^{-(k_r+k_{nr})t} dt = \frac{k_r}{k_r + k_{nr}} = \Phi \quad (2)$$

So we see that the quantum yield can also be interpreted as the amount of radiative emissions per excitation. Another important quantity is the molar extinction coefficient ϵ . It is defined as the factor by which the intensity of light is reduced by a substance, divided by the pathlength and the molar concentration. Together with the quantum yield it determines the brightness of a fluorophore. Obviously in fluorescence experiments we want our fluorophores to be as bright as possible.

The last thing we need to discuss are the excitation and emission axes of fluorophores. A fluorophore absorbs light more efficiently if its polarization is parallel to the excitation axis, and it emits light more efficiently with a polarization parallel to the excitation axis. These axes are also called transition dipole moments. For both excitation and emission, we can imagine the amplitude of the light being projected onto the respective transition dipole moment. This yields an efficiency factor of $\cos(\theta)$, where θ is the angle between the the polarization of the light and the axis. Because the intensity of light is proportional to the square of the amplitude, this means that the transition probabilities are proportional to $\cos^2(\theta)$. The relative orientation of the transition dipole moments depends on the wavelength of the light and the electrical structure of the fluorophore, although generally the excitation and emission transition dipole moments are assumed to be parallel.

2.2 FRET

FRET (short for Förster Resonance Energy Transfer) is the process whereby an excited fluorophore transfers its energy to another nearby fluorophore. It is important to note that this process is non-radiative and happens via an electric process which is similar to resonance in a mechanical system. The

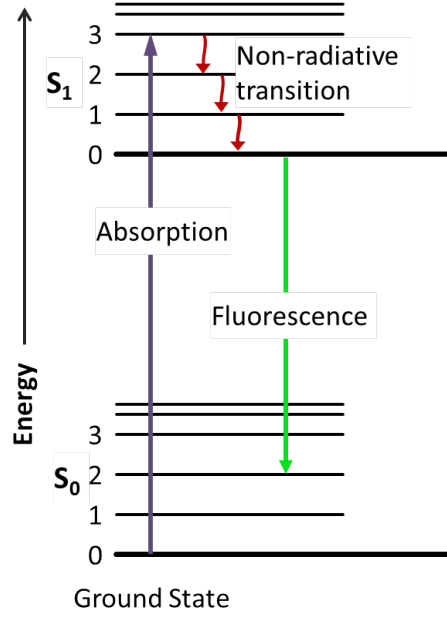


Figure 1: Jablonski diagram of a typical fluorescence process.

fluorophore that transfers the energy is called the donor and the fluorophore that receives it is called the receptor. In general, these are different kinds of molecules (hetero-FRET), but they can also be the same kind (homo-FRET). The rate of energy transfer k_T is given by:

$$k_T = k_D \left(\frac{R_0}{r} \right)^6 \quad (3)$$

Here k_D is the total decay rate of the donor in the absence of a fluorophore, r is the distance between the fluorophores, and R_0 is the Förster distance (typically on the order of 1-10 nm). Note that when $r = R_0$, $k_T = k_D$ and so exactly half of the excitation energy of the donor will be transferred, and the other half will vanish due to normal decay processes (on average). The Förster distance depends on many factors and is given by:

$$R_0^6 = \frac{9000 \ln(10) \kappa^2 \Phi_D}{128 \pi^5 N n^4} \int_0^\infty F_D(\lambda) \epsilon_a(\lambda) \lambda^4 d\lambda \quad (4)$$

Here Φ_D is the quantum yield of the donor, n is the refractive index of the medium, N is Avogadro's number, κ is an orientation-dependent factor, $F_D(\lambda)$ is the emission intensity of the fluorophore as a function of the wavelength (so basically the emission spectrum of the donor), and $\epsilon_a(\lambda)$ is the absorption spectrum of the acceptor. The last term is a measure of the spectral overlap between the donor and acceptor molecules. We see that once a setting (donor, acceptor and medium) has been chosen, the energy transfer efficiency is only dependent on the distance and mutual orientation between the fluorophores.

2.3 Anisotropy

Because of the fact that light is not absorbed and emitted isotropically by a fluorophore (because of the transition dipole moments), the light coming from a fluorophore will generally be polarized. Consider a normal Cartesian (x, y, z) -coordinate system. If we shoot a beam of light in the x -direction, polarized in the z -direction, into a sample of fluorophores, the emitted light intensity will have a parallel (I_{\parallel}) and

a perpendicular component (I_{\perp}) (relative to the z-axis). Actually, there should be two perpendicular components: I_x and I_y , but if we assume that the fluorophore has parallel excitation and emission axes, these are equal because of the symmetry of the system. Therefore the total intensity is $I = I_x + I_y + I_z = 2I_{\perp} + I_{\parallel}$. Now, one measure of the polarization of the emission is P , which is given by:

$$P = \frac{I_{\parallel} - I_{\perp}}{I_{\parallel} + I_{\perp}} \quad (5)$$

However, it is more practical to use the polarization anisotropy r , which is defined as:

$$r = \frac{I_{\parallel} - I_{\perp}}{I_{\parallel} + 2I_{\perp}} \quad (6)$$

This is because r has some nice properties. For example, when we have 2 fluorophores A and B with anisotropies r_A and r_B and relative intensities f_A and f_B , the total anisotropy r_{A+B} will simply be:

$$r_{A+B} = f_A r_A + f_B r_B \quad (7)$$

As can easily be checked from the definition of r and the total intensity. Note that when the emission is completely polarized ($I_{\perp} = 0$), the anisotropy is 1, and when the emission is completely depolarized ($I_{\parallel} = 0$), it is $-\frac{1}{2}$. Also note that the anisotropy does not vary with varying total intensity.

2.3.1 A single molecule

We are now ready to calculate the anisotropy of a single, static fluorophore molecule, in an isotropic solution. This means that it has a random orientation which is constant in time. We assume that the excitation and emission transition dipole moments are parallel to each other. Consider again a beam of light, polarized in the z-direction, which hits the solution. Consider one of the fluorophores in the solution. Its transition dipole moment will have some orientation relative to our (x, y, z) -coordinate system. This orientation can be parametrized by two angles θ and ϕ , as in figure 2.

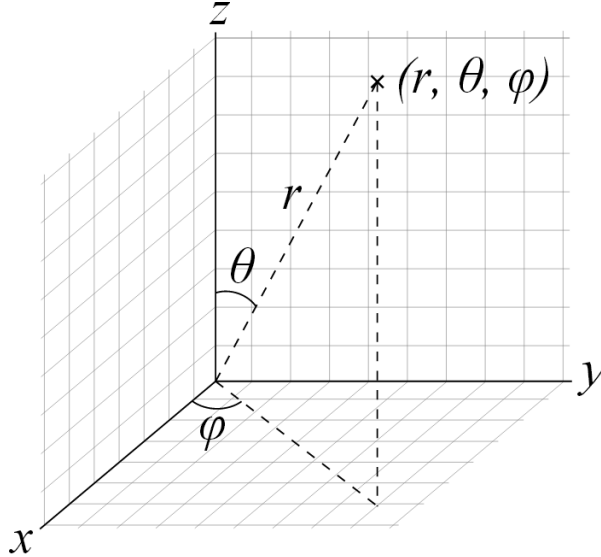


Figure 2: A representation of the spherical coordinate system we use. The transition dipole moment would be represented by the line between the origin and the marked point. Since we are only concerned with the orientation of the transition dipole moment, we will always choose r to be 1.

The projections of the transition dipole moment onto the z-axis and the x-axis are $\cos(\theta)$ and $\sin(\theta)\sin(\phi)$. This means that the part of the excitation light intensity that is absorbed is proportional to $\cos^2(\theta)$.

The parallel part of the emitted light intensity is proportional to $\cos^2(\theta)$ and the perpendicular part is proportional to $\sin^2(\theta)\sin^2(\phi)$. You could say that the "odds" that a photon makes it through a path (being absorbed, being emitted, going through an imaginary polarization filter in either the parallel or perpendicular direction) is equal to the odds that it survives both projections. Therefore, we can say that:

$$I_{\parallel} \propto \cos^2(\theta)\cos^2(\theta) = \cos^4(\theta) \quad (8)$$

$$I_{\perp} \propto \cos^2(\theta)\sin^2(\theta)\sin^2(\phi) \quad (9)$$

This is all for a specific orientation of the fluorophore. Since the solution is isotropic, the fluorophore could have any orientation with equal probability. We can find the average parallel and perpendicular intensities of a randomly oriented fluorophore by integrating 8 and 9 over all possible orientations:

$$\begin{aligned} I_{\parallel,av} &\propto \frac{1}{4\pi} \int_0^{\pi} \int_0^{2\pi} \cos^4(\theta) \sin(\theta) d\phi d\theta = \frac{1}{5} \\ I_{\perp,av} &\propto \frac{1}{4\pi} \int_0^{\pi} \int_0^{2\pi} \cos^2(\theta) \sin^2(\theta) \sin^2(\phi) \sin(\theta) d\phi d\theta = \frac{1}{15} \end{aligned} \quad (10)$$

Note that the Jacobian $\sin(\theta)$ is present because we are integrating in spherical coordinates. We can now calculate the anisotropy r_1 of a single, randomly oriented molecule, using equation 6:

$$r_1 = \frac{\frac{1}{5} - \frac{1}{15}}{\frac{1}{5} + 2\frac{1}{15}} = \frac{2}{5} = 0.4 \quad (11)$$

This is an important result. It tells us that the maximum anisotropy of light emitted from an isotropic sample of fluorophores is 0.4. It is maximal because all other factors which affect anisotropy (which we will discuss later) have a lowering affect. Note that in the entire derivation we only considered the light that was absorbed, and subsequently released via a radiative decay process. Of course, there is a lot of light that does not get absorbed, and not all excited fluorophores actually decay radiatively. However, the excitation light has a different wavelength than the emitted light, and is filtered out in an actual experiment. So in an experiment we only measure the light that has actually been emitted from a fluorophore, and it is this light which we use to determine the anisotropy.

2.3.2 Two molecules

What happens to the anisotropy of a solution when the molecules get close enough for FRET to occur? In this section we consider the expected anisotropy of two identical, randomly oriented fluorophores, which are in close proximity to each other and which exhibit homo-FRET. We assume that at time $t = 0$ fluorophore number one is excited, and neither fluorophore 1 nor 2 is excited again during the fluorescence process. We can split the problem up into two parts: "How many photons do we expect from fluorophore 1 and fluorophore 2?", and, "What are the expected anisotropies from fluorophore 1 and fluorophore 2?". To answer the first question, we need to write down the differential equations for the probabilities that the fluorophores are excited as a function of time t . We shall call the probabilities that fluorophore 1 and 2 are in the excited state $\rho_1(t)$ and $\rho_2(t)$. The change in the probability that a fluorophore is excited is simply the sum over all the rates that either excite it or make it decay. Therefore we get the following set of coupled differential equations (with boundary conditions):

$$\begin{aligned} \dot{\rho}_1 &= -k\rho_1 - F\rho_1 + F\rho_2 & \rho_1(0) &= 1 \\ \dot{\rho}_2 &= -k\rho_2 - F\rho_2 + F\rho_1 & \rho_2(0) &= 0 \end{aligned} \quad (12)$$

Here k is the total decay rate of the fluorophore (radiative and non-radiative), and F is the FRET rate between the fluorophores (obviously the rate from 1 to 2 is equal to the rate from 2 to 1, since the

fluorophores are identical). These are two coupled first order differential equation, and luckily there is an exact solution, given by:

$$\begin{aligned}\rho_1(t) &= \frac{1}{2}e^{-kt}\left(1 + e^{-2Ft}\right) \\ \rho_2(t) &= \frac{1}{2}e^{-kt}\left(1 - e^{-2Ft}\right)\end{aligned}\tag{13}$$

We can now calculate the expected number of emitted photons from both fluorophores, Φ_1 and Φ_2 :

$$\begin{aligned}\Phi_1 &= \int_0^\infty k_r \rho_1(t) dt = \int_0^\infty \frac{1}{2} k_r e^{-kt} (1 + e^{-2Ft}) dt = \frac{k_r(F+k)}{k(2F+k)} \propto \frac{F+k}{2F+k} \\ \Phi_2 &= \int_0^\infty k_r \rho_2(t) dt = \int_0^\infty \frac{1}{2} k_r e^{-kt} (1 - e^{-2Ft}) dt = \frac{k_r F}{k(2F+k)} \propto \frac{F}{2F+k}\end{aligned}\tag{14}$$

Now that we have answered question one, we can calculate the total anisotropy r_2 of the system using equation 7:

$$r_2 = \frac{F+k}{2F+k} r_1 + \frac{F}{2F+k} r_{et}\tag{15}$$

Here r_1 is the anisotropy of fluorophore 1, which is simply equal to the anisotropy of a randomly oriented fluorophore (see section 2.3.1). The anisotropy of a randomly oriented fluorophore *that got its excitation from another randomly oriented fluorophore through FRET* is r_{et} , and is a bit more complicated. Suffice it to say it is equal to 0.016 (we will calculate it later) and therefore:

$$r_2 = \frac{F+k}{2F+k} 0.4 + \frac{F}{2F+k} 0.016\tag{16}$$

Often, because r_{et} is so small, it is simply assumed to be zero. Note that when F is very large compared to k (i.e. when the fluorophores are very close), the anisotropy goes to $(0.4+0.016)/2 \approx 0.2$. This makes sense, as in this case both fluorophores have an approximately equal chance of emitting a photon.

2.3.3 Calculating r_{et}

Calculating r_{et} is similar to calculating r_1 . Now, the path that a photon has to go through to become a parallelly polarized photon is as follows: be absorbed by fluorophore 1, be transferred to fluorophore 2, be emitted with parallel polarization by fluorophore 2. A perpendicularly polarized photon follows the same path, except the last step is "be emitted with perpendicular polarization by fluorophore 2". The orientations of fluorophore 1 and 2 are parametrized by θ_1, ϕ_1 and θ_2, ϕ_2 . The orientation of the line connecting both fluorophores is parametrized by θ_3, ϕ_3 . Just as in the derivation of r_1 , we assume that the excitation light is polarized in the z -direction. We already know the probabilities for steps 1 and 3 in the paths, but not yet for step 2. When we look at equation 4, we see that the probability of energy transfer is proportional to the orientation factor κ^2 . This factor is given by:

$$\kappa = v_1 \cdot v_2 - 3(v_1 \cdot v_3)(v_2 \cdot v_3)\tag{17}$$

Where $v_{1,2,3}$ are the unit vectors describing the orientations of fluorophore 1, fluorophore 2, and the connection line respectively. Now we know the probability of all three steps in the each path. We can calculate the expected number of parallelly and perpendicularly polarized photons from fluorophore 2 by integrating the product of these step probabilities over all possible orientations of 1, 2 and 3. To do this we must first write out κ in terms of θ 's and the ϕ 's. We can do this using the expression for the inner product in spherical coordinates. This gives us the following horrific expression:

$$\kappa = s(\theta_1)s(\theta_2)c(\phi_1 - \phi_2) + c(\theta_1)c(\theta_2) - 3s(\theta_1)s(\theta_3)c(\phi_1 - \phi_3) + c(\theta_1)c(\theta_3)s(\theta_2)s(\theta_3)c(\phi_2 - \phi_3) + c(\theta_2)c(\theta_3)\tag{18}$$

Where s stands for a sine and c stands for a cosine. Now we can calculate the parallel and perpendicular intensities:

$$\begin{aligned} I_{\parallel,av} &\propto \frac{1}{(4\pi)^3} \left(\int_0^\pi \int_0^{2\pi} \right)^3 c^2(\theta_1) \kappa^2 c^2(\theta_3) s(\theta_1) s(\theta_2) s(\theta_3) d\phi_1 d\theta_1 d\phi_2 d\theta_2 d\phi_3 d\theta_3 \approx 0.0764527 \\ I_{\perp,av} &\propto \frac{1}{(4\pi)^3} \left(\int_0^\pi \int_0^{2\pi} \right)^3 c^2(\theta_1) \kappa^2 s^2(\theta_3) s^2(\phi_3) s(\theta_1) s(\theta_2) s(\theta_3) d\phi_1 d\theta_1 d\phi_2 d\theta_2 d\phi_3 d\theta_3 \approx 0.0728989 \end{aligned} \quad (19)$$

These integrals have been evaluated numerically using *Mathematica*. Using these parallel and perpendicular intensities we can calculate the expected anisotropy:

$$r_{et} = \frac{I_{\parallel,av} - I_{\perp,av}}{I_{\parallel,av} + 2I_{\perp,av}} \approx 0.01599 \quad (20)$$

This agrees well with the value $r_{et} = 0.016$ found in literature [4] [5]. Notice that $r_{et} = \left(\frac{2}{5}\right)^2 = r_1^2$. Further numerical calculations seem to indicate that the anisotropy of light that has been transferred through multiple randomly oriented fluorophores is equal to r_1^n , where n is the number of fluorophores involved. However since even after a single energy transfer the remaining anisotropy is often considered negligible, this doesn't have any impact on actual anisotropy calculations.

2.3.4 Generalization

The method for determining the anisotropy of two molecules interacting via homo-FRET can be extended to larger clusters of molecules. Assume that we have N randomly oriented fluorophores in a cluster, and that at time $t = 0$, fluorophore number 1 is excited. Again we can split the problem into determining the expected quantum yield of each fluorophore, and determining the anisotropy from each of the fluorophores. The first question is again solved by a partial differential equation. Call $\rho_i(t)$ the probability that fluorophore i is excited at time t . Then we get:

$$\dot{\rho}_i = -k\rho_i + \sum_{j=1}^N \left(-F_{ij}\rho_i + F_{ji}\rho_j \right) \quad \rho_i(0) = \delta_{1,i} \quad (21)$$

Where δ is the Kronecker delta function, and $F_{i,j}$ is the FRET rate from molecule i to molecule j . Since we are dealing with homo-FRET, clearly $F_{i,j} = F_{j,i}$. This differential equation can be rewritten as a first order matrix differential equation and subsequently solved numerically or exactly with some tricks. In the special case of a cluster where all the fluorophores interact equally (i.e. all the relative distances are equal), we can say that $F_{i,j} = F$ and the following exact solution exists:

$$\begin{aligned} \rho_1(t) &= \frac{1}{N} e^{-kt} (1 + (N-1)e^{NFt}) \\ \rho_{i,i \neq 1}(t) &= \frac{1}{N} e^{-kt} (1 - e^{NFt}) \end{aligned} \quad (22)$$

This gives the following quantum yields:

$$\begin{aligned} \Phi_1 &= \frac{k_{nr}(F+k)}{k(NF+k)} \propto \frac{F+k}{NF+k} \\ \Phi_{i,i \neq 1} &= \frac{k_{nr}F}{k(NF+k)} \propto \frac{F}{NF+k} \end{aligned} \quad (23)$$

This gives us the following expected anisotropy:

$$r_N = \frac{F+k}{NF+k}r_1 + (N-1)\frac{F}{NF+k}r_{et} \quad (24)$$

We see that in the limit of a large cluster ($N \rightarrow \infty$), the anisotropy goes to r_{et} , so roughly to zero. Also, in the limit of efficient FRET ($F \rightarrow \infty$), we see that the anisotropy goes to $\frac{1}{N}r_1 + \frac{N-1}{N}r_{et}$, so roughly to $\frac{1}{N}r_1$.

2.4 Polarization affecting factors

2.4.1 Rotational diffusion

So far we have assumed that the fluorophores remain stationary during the whole fluorescence process. Because of thermodynamics however any small object (such as a molecule) will experience rotation due to thermal energy. The rate of this rotation is characterized by the rotational correlation time θ . This is the typical timescale on which a molecule will change its orientation significantly. This means that the larger θ is, the smaller the rate of rotation will be. The value of θ depends heavily on the size of the molecule, the temperature, and the medium it's in. For a spherical molecule we have the following equation [3]:

$$\theta = \frac{\eta V}{RT} \quad (25)$$

Where η is the viscosity of the medium, V is the approximate volume of the molecule, R is the gas constant and T is the temperature. Typical values of θ vary over several order of magnitude, but it is generally around the nanosecond scale. When a fluorophore is excited by polarized light, it will generally be oriented in the polarization direction. This is what causes the expected anisotropy of the emission. When the fluorophore rotates significantly in the time that the fluorophore is excited, naturally the anisotropy will decrease. How much the anisotropy of a single molecule decreases is given by the Perrin equation [3]:

$$r(t) = r_0 e^{-t/\theta} \quad (26)$$

Where $r(t)$ is the anisotropy at time t , and r_0 is the anisotropy at $t = 0$. We can calculate the average anisotropy r_l by integrating equation 26 over all time. This must of course be weighted by the expected radiative emission rate at time t :

$$r_l = \frac{\int_0^\infty r(t) k_r e^{-kt} dt}{\int_0^\infty k_r e^{-kt} dt} = \int_0^\infty r_0 e^{-t/\theta} k e^{-kt} dt = \frac{r_0}{k + 1/\theta} = \frac{r_0}{1 + \tau/\theta} \quad (27)$$

Where k and τ are the fluorophore's total decay rate and lifetime respectively. From this expression it is clear that when $\theta \gg \tau$, the rotational diffusion has no significant effect on the anisotropy, but when $\theta \approx \tau$, it does. When $\theta \ll \tau$, the anisotropy drops to zero, and the emission is totally depolarized. The polarization decreasing factor in equation 27 can also be used in the case of FRET. For large values of θ it is approximately valid to simply attach the decay factor to the expected anisotropy. The general equation for the expected anisotropy of a cluster of N molecules then becomes:

$$r_{N,rotdif} = \frac{r_N}{1 + \tau/\theta} \quad (28)$$

2.4.2 Non-parallel excitation/emission axes

It is possible that the excitation and emission axes of a fluorophore are not parallel. This decreases the anisotropy because now even a fluorophore that is oriented perfectly parallel to the excitation polarization will on average not emit parallel to the excitation polarization. Call the angle between

the excitation and emission transition dipole moments β . Then the anisotropy of a single molecule is changed to [3]:

$$r = 0.4 \frac{3\cos^2(\beta) - 1}{2} \quad (29)$$

In combination with FRET, the effect of non-parallel excitation/emission axes becomes more complicated, as the alignment affects not only the anisotropies of the fluorophores, but also the rate of FRET itself. Just as in the case with rotational diffusion though, if the effect is small, we can reasonably approximate the anisotropy with FRET simply by multiplying the original value with the decreasing factor. Fortunately equation 29 is quite forgiving for small angles. To decrease the anisotropy of a single molecule to 0.39 a non-parallel-ness of 7.4 degrees is needed. What makes it even more complicated is that the misalignment is in general dependent on the excitation wavelength. Shorter excitation wavelengths lead to more misalignment, since the excited fluorophore will have a lot of energy and thus have many possible emission axes to choose from.

2.5 Protein clustering

Now that we have discussed the basic concepts in FRET-microscopy we are ready to think about measuring protein clustering. The basic idea is to measure an anisotropy map of a cell in which some type of protein has been labeled by a fluorophore. When protein clustering is present, the fluorophores will be close together and FRET will occur, which lowers the anisotropy. So basically in any area with a lowered anisotropy we can say that some kind of clustering of our target protein has occurred. Of course, to measure the anisotropy decrease we must first know the anisotropy of the fluorophore when no clustering is present. This can be done by measuring the anisotropy of an unclustered solution of the fluorophore in a similar medium. An unclustered solution is generally achieved simply by taking a low concentration of the fluorophore. It is however possible that the fluorophore clusters even at very low concentrations (simply because it is chemically favored). Therefore some information about the clustering of the fluorophore is needed before it can be used. The tendency for a protein to cluster is specified by its so called dissociation constant K_d . For dimerization this constant is the concentration at which we have equal concentration of monomers and dimers. We need the concentration of our protein to be much less than K_d in order for clustering to be negligible. After determining the anisotropy without clustering, we can start measuring the anisotropy in our samples to determine their protein clustering. With accurate measurements of the anisotropy, it might be possible to determine the size of the clusters, because we have seen that a larger cluster size decreases the anisotropy further. The difficulty with this however is that it requires accurate anisotropy values for every cluster size. These can be calculated theoretically, but this requires information about the structure of the clusters. If there are many possible structures for a certain cluster size (as is likely to be the case with complex proteins), theoretical calculations become unreliable, and the only real way to determine the anisotropy of clusters is by reference measurements performed on a fluorophore-protein sample with known cluster sizes. One way to do this would be using PAGE (PolyAcrylamide Gel Electrophoresis) analysis. Samples with varying amounts of clustering could be prepared. The relative amounts of each cluster size could be determined via PAGE, and then measurements of the anisotropy of each sample would give the anisotropy of each cluster size.

2.6 Measuring anisotropy: T-setup vs. L-setup, Steady-state vs. Time-resolved, Wide-field vs. Confocal

How do we actually measure anisotropy? We need to excite our sample with polarized light with a wavelength that lies inside the excitation spectrum. Then fluorescence will occur and we get some light back. Part of this light will be from fluorescence and part of it will be from reflections. We can filter out the reflections by only allowing light which lies in a part of the emission spectrum that does not overlap with our excitation spectrum. Now that we have the fluorescence light we need to split it up into its parallel and perpendicular components (relative to the excitation light). This can be achieved by a simple set of polarization filters. We can measure the parallel and perpendicular components at

the same time by using a polarizing beam splitter (PBS) and two cameras. We can also measure them one by one, simply by using one camera and a rotatable polarization filter. The first method is called the T-method and the second method the L-method (a reference to the actual shape of such a setup). The T-method provides faster measurement (because we measure two images at once), and is the only option when the sample changes in time. It does however require some sort of post-measurement data processing to align the images from both cameras (something that we'll discuss later), whereas in an L-setup both images are automatically aligned. In our experiment we chose to use a T-setup, because of the easier measurement process. Furthermore there is a choice between steady-state and time-resolved measurement. In steady state measurement, the sample is illuminated continuously during imaging. The imaging time is much larger than the timescale of the fluorescence process, so we get an averaged out value of the anisotropy. In time-resolved measurement, the excitation light is pulsed, and after every pulse the emission anisotropy is measured as a function of time. The pulse is as short as possible, and the time in between the pulses has to be large enough to allow all fluorophores to completely decay before the next excitation. With the anisotropy as a function of time, the FRET rate can be determined, and hence something can be said about cluster size. An advantage of this method is that it can also be used to measure the rotational diffusion rate of fluorophores. It is however, a more time-consuming method and it requires more complicated data-analysis. Considering this and the fact that the rotational diffusion times of most fluorophores are known (or can be estimated), we decided to go with the steady state method. Another method altogether is FLIM (Fluorescence lifetime imaging microscopy). This method also uses pulsed excitation light, but only measures the intensity of the emission of the donor fluorophore instead of the anisotropy. Using this, the excitation decay rate of the donor can be determined. When FRET occurs, the donor will lose its excitation to the receptor fluorophore, whose emission is not measured. Therefore, the intensity will decay faster. Obviously, this method only works if the donor and receptor fluorophores are different, so this was not an option for us. A third important choice was between wide-field and confocal microscopy. In wide-field microscopy, the whole sample is illuminated at the same time with a large imaging depth, yielding more light but fuzzier images. In confocal microscopy, a thin layer of the sample is imaged one point at a time, which yields better depth-resolution and contrast at the cost of brightness. Also, because every point in the same has to be illuminated separately, this method is very time consuming. For our experiments we chose wide-field, since it yields more light, and measurements are a lot faster.

2.7 Some numbers

In this section we will give some relevant information about the fluorophores we use in this experiment. We will be measuring in the red and the green part of the spectrum. For each part we need a small fluorescent dye and a large fluorescent protein. The dyes we have chosen are rhodamine-B and fluorescein. Both are well-documented fluorescent dyes that have been used for decades. The proteins we have chosen are GFP (Green Fluorescent Protein) and mCherry (the m stands for monomeric). Both of these are very well known in the field of microscopy. The structures of these fluorophores are shown in figure 3. The values of some important parameters are shown in table 1. As an addendum the homo-FRET Förster distance for GFP is 4.65 nm [20] and for mCherry 5.10nm [21]. Many of these numbers were important factors in deciding which fluorophores to use. For all the fluorophores it was important that they were generally monomeric, and that their excitation and emission wavelengths were suitable for our red and green dichroic cubes. For our dyes we wanted the rotational diffusion time to be low relative to the fluorescence lifetime, and for the proteins we wanted it to be high. Furthermore, the brightness of the proteins is of key importance to combat the influence of autofluorescence on anisotropy measurements in cells [1].

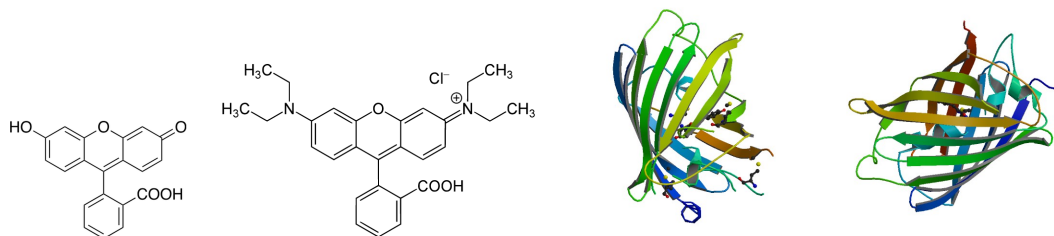


Figure 3: The structures of the fluorophores we used. From left to right: fluorescein, rhodamine-B, GFP, mCherry. The last two images were taken from the RCSB Protein Data Bank.

Fluorophore	EX	EM	QY	Ext. Coef.	Bright	Photo	LF	RC
Fluorescein	495 [14]	517 [14]	0.79 [7]	92000 [7]	73	5.2 [9]	4 [14]	0.2*
Rhodamine-B	562 [14]	583 [14]	0.7 [7]	106000 [7]	74	$>10^\dagger$	2 [14]	0.2 [12]
EGFP	488 [9]	507 [9]	0.6 [10]	56000 [10]	34	174 [9]	3 [13]	20 [11]
mCherry	587 [9]	610 [9]	0.22 [10]	72000 [10]	16	96 [9]	1.5 [15]	20*

Table 1: Some information about the fluorophores we used in this experiment. EX = excitation peak (in nm). EM = emission peak (in nm). QY = quantum yield. Ext. Coef. = extinction coefficient (in $\text{mol}^{-1} \text{ cm}^{-1}$). Bright = brightness (product of QY and Ext. Coef. divided by 1000). Photo = photostability (time to reduce intensity by factor of 2 in s). LF = lifetime (in ns). RC = rotational correlation time (in ns) in water. Please note that many of these values are heavily dependent on specific experimental conditions, such as temperature and the solvent of the fluorophore. Therefore most of these values should be taken as a rough estimate of the "general" value. *These rotational diffusion times were extrapolated from the other two under the assumption that they would be roughly the same for similarly sized molecules. \dagger Based on own observations.

3 Experimental setup

As discussed in section 2.6, we will be using a T-setup for this experiment. To describe the components of the setup, let us follow a beam of light through it:

- *Mercury lamp.* Light is generated in a short-arc mercury lamp. Mercury lamps have a very broad spectrum with strong peaks and are therefore very flexible in their purpose.
- *Excitation polarizer.* The light passes through a linear polarizer before entering the microscope. The polarizer is a Thorlabs WP25L-UB Ultra-Broadband 25x25mm wire grid polarizer which works for light with a wavelengths between 250nm and 4000nm. It has roughly 75% transmission and an extinction ratio of over 5000 for our wavelengths.
- *Microscope.* The light enters the microscope and is reflected towards the center by a mirror. The microscope is a Nikon Ti Epsilon which can hold 6 different objectives and dichroic cubes.
- *Dichroic cube.* The light hits a dichroic cube. Dichroic cubes consist of three parts: a dichroic mirror in between two different bandfilters. The first band-filter is used to select the excitation wavelength band. Then the light hits the dichroic mirror. This mirror has a certain characteristic wavelength. Only light with a wavelength which is lower than this characteristic wavelength is reflected up into the objective. The rest passes through and is absorbed by some microscope wall.
- *Objective.* The light goes through an objective which focuses the light onto the sample. In our setup we use a Nikon S Plan Fluor which has a numerical aperture of 0.6 and a magnification of 40x. Some of the light is absorbed by the sample and causes fluorescence. Another part is simply reflected. Some of the light from both parts comes back into the objective and is sent to the dichroic.
- *Dichroic cube.* The light hits the dichroic mirror again. The part of the light with a wavelength lower than the characteristic wavelength is reflected, and subsequently absorbed by a wall, while the part of the light with a higher wavelength is let through. Therefore only light from fluorescence (which has a higher wavelength) is allowed to continue. The light that was let through by the mirror then passes through a second band-filter which again ensures that only the light from fluorescence is let through. The light is reflected and exits the microscope, into the T-shaped part of the setup.
- *Primary lens.* Since the microscope is built for direct camera attachment, the light will be focussed about 17mm after exiting the microscope. In order to prepare the light for the polarizing beam splitter, the light is made parallel (as in not converging or diverging) by an achromatic doublet lens (Thorlabs, AC-508-080-A-ML), which has a focal length of 80mm.
- *Polarizing beam splitter.* The light hits the polarizing beam splitter (PBS). This splits the light into a parallelly and a perpendicularly polarized part. The parallel part continues unhindered but the perpendicular part is reflected to the right. The model of the PBS is Thorlabs CM1-PBS-251. Its extinction ratios have been measured to be 1000 and 40 for the parallel and the perpendicular part respectively [1]. Since the extinction ratio of 40 is somewhat poor, another linear polarizer was added in the perpendicular path.
- *Secondary lenses.* The light now needs to be focussed onto the cameras. This is accomplished by two more lenses of the same type as the first lens.
- *Extra polarizer* A second linear polarization filter is added in the perpendicular path (behind the second lens), to compensate for the poor extinction ratio of the PBS. It is a Thorlabs WP25M-VIS 420-700 nm wiregrid polarizer, which has a transmission of roughly 90% and an extinction ratio of about 300 for our wavelengths.
- *Cameras.* Finally, the light is focused onto the imaging chips of the cameras. The model of both cameras is Andor sCMOS Neo 5.5. We will be describing the cameras in more detail later.

A schematic representation of the setup is shown in figure 4. The path the light goes through before hitting the sample is called the excitation path, and the path after coming from the sample the emission path. We will now go into a bit more detail about some parts of the setup.

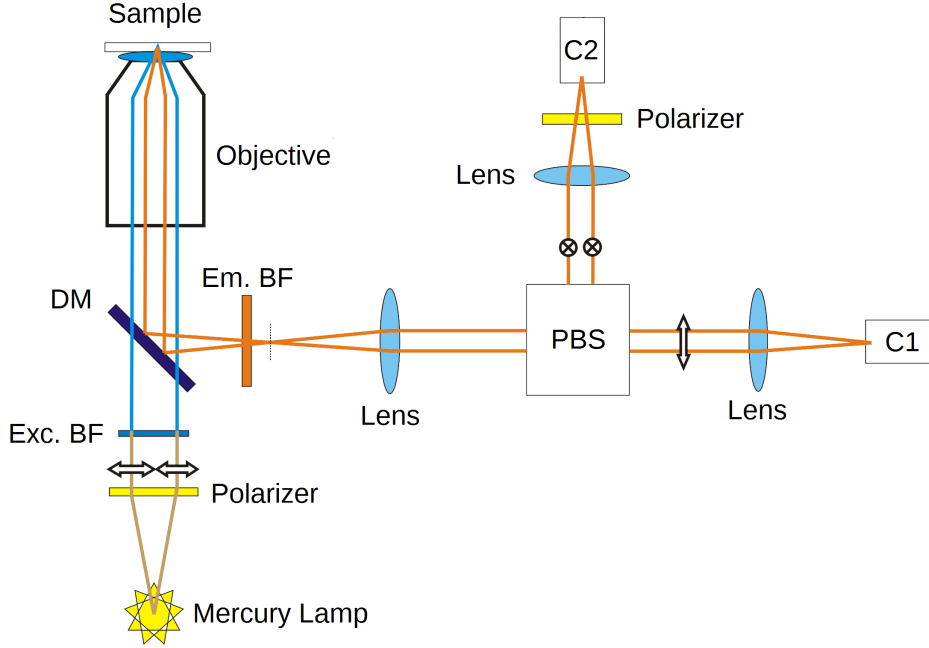


Figure 4: A schematic representation of our setup. DC = dichroic mirror, Exc. BF = excitation bandfilter, Em. BF = emission bandfilter, PBS = polarizing beam splitter, C1/C2 = Camera1/Camera2. Light with a high wavelength is colored red, and light with a low wavelength blue. Also, at several points the polarization of the light is indicated. Note that the behaviour of the dichroic mirror in this schematic is the opposite of its actual behaviour. The dichroic actually lets through light with a high wavelength, and reflects light with a low wavelength. Nonetheless the principle remains the same and the rest of the schematic is accurate.

3.1 The dichroic cubes

In our description of the setup we left out the specifications of our dichroic cube. This is because we actually use three different dichroic cubes. The first one (which we will call dichroic A), is the one that Nivard Kagie [1] used for his experiments. It is suitable for microscopy with GFP. We will be using this one mainly for reference measurements to compare things like the autofluorescence of cells in the red and the green part of the spectrum. Dichroic B is a generic red dichroic that can be used for imaging mCherry and rhodamine. We used this dichroic mostly for reference measurements as well. Finally we have dichroic C, which is specialised for use with mCherry, and which we plan to use for the final anisotropy measurements of the mCherry labeled cells. The reason many of the reference measurements were done with dichroic B instead of C is that dichroic C had to be ordered and came quite late. Specifications of all three dichroic cubes can be seen in table 2).

	Excitation filter	Dichroic mirror	Emission filter
Dichroic A	460-500	505	516-556
Dichroic B	510-560	575	590- ∞
Dichroic C	540-580	585	590-670

Table 2: Specifications of the three dichroic cubes we use in our setup. The part of the spectrum that is let through by the excitation and emission band filters is given, as well as the characteristic wavelength of the dichroic mirror. All values are in nm.

3.2 The cameras

As mentioned before both cameras are Andor sCMOS Neo 5.5. They are sensitive primarily to visible and NIR light (400-1000nm), as can be seen in figure 5. Note that the camera is slightly more sensitive to mCherry than to GFP. The light-sensitive chip has 2560x2160 pixels, each measuring $6.5\mu\text{m} \times 6.5\mu\text{m}$. Since the magnification of the microscope is 40x this means that every pixel represents about 160nm in the sample. The chip has a diagonal of 22mm and is held in a vacuum chamber, where it can be cooled down to -40 °C. The cameras are connected to a computer, which receives the images and controls the cameras. Before we go any further we must first discuss how the chip works. Every pixel has a sensor, which can convert light into electron-hole pairs, which is then turned into a voltage. Every row of the chip has two amplifiers which amplify this voltage, before sending it to two separate A/D (analog to digital) converters, which convert all the voltages in the row to a digital signal. The two amplifiers amplify the voltage by different factors (so called gain factors), and after conversion to two separate 11-bit signals these are recombined to create a single 16-bit signal. This signal is then sent to the computer, where it is used to create an image. Every pixel produces a 16-bit signal, so every pixel has a 65536 possible grayscale values. Now, there are two ways in which the camera can read out the rows:

- *Global shutter* Charge is accumulated in each pixel during the exposure time. The exposure starts and stops at exactly the same time for all pixels. Afterwards, all rows are read out.
- *Rolling shutter* The rows are read out sequentially, two rows at a time, starting from the middle two rows and moving outwards. This happens at a rate of 560 MHz (280MHz x two rows at a time, pixels per second). Since there are 2560 pixels per row, reading out each row takes about 10 μs . There are 1080 rows per half, so reading out the entire image will take about 1 ms. This means that rolling shutter is not suitable for samples which change significantly on the millisecond timescale (you will get smearing of the target object). However, the rolling shutter method produces about three times as much signal, while the fundamental background level is the same as with global shutter. We suspect that the rolling shutter mode yields more signal because a larger gain factor (amplification factor) is used.

Considering the fact that rolling shutter produces relatively less noise and more signal than global, and the fact that our samples don't move significantly, we decided to use the rolling shutter method. Furthermore, in the imaging software, it is possible to select a region we want to image. We chose to use only the middle 500x500 pixels, as this saves storage space and easily accommodates a cell. Also, this makes the image alignment more accurate, since we optimize the warping and skewing for this section of the image only.

3.3 Alignment

The setup has several degrees of freedom in positioning the cameras, the PBS, and the lenses. The cameras and PBS are mounted directly to the optical table for extra stability and fewer degrees of freedom (making use of the precision of the table). The lenses are supported by lens tubes which span the distance between the PBS and the cameras/microscope. These lens tubes can still be rotated (screwed), to allow for fine positioning of the lenses. To make sure that the light passes through the PBS in a parallel way, the distance between the primary lens and the focus of the microscope needs to be 80mm. Similarly, to ensure a sharp image the distances between two secondary lenses and the camera chips need to be 80mm as well. Also, less obviously, it is recommended to make sure that the distance between all three lenses and the PBS is also 80mm. This reduces spherical and chromatic aberration. In our final setup, the distances of the three lenses to the PBS were 81, 81 and 89mm respectively. Since the PBS itself is a cube with a thickness of over 20mm, these deviations are acceptable. The distances between the lenses and the cameras/focus of the microscope need to be set precisely. It has been determined that the depth of focus of our lenses is approximately 0.2mm [1]. This is actually quite easily achievable because of the screw-method. The cameras are mounted to the table with two post-holders each, making (in principle) only the height adjustable. The table will ensure (in principle) that the cameras are oriented properly in the other five degrees of freedom. The PBS is mounted in

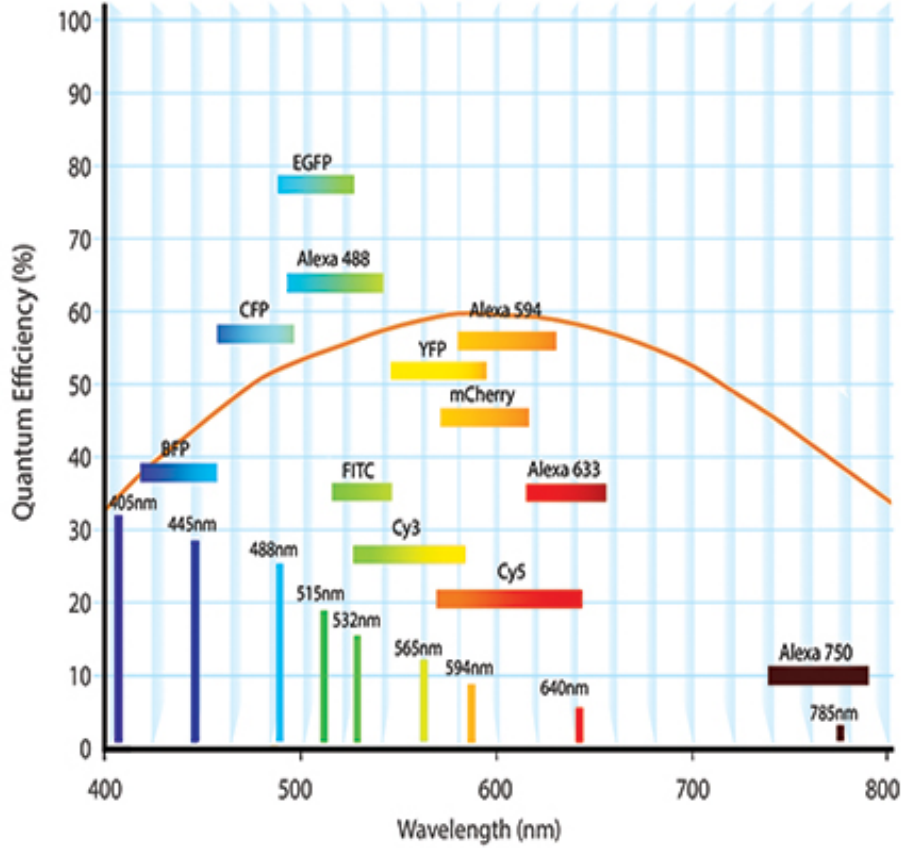


Figure 5: A graph displaying the sensitivity of the Andor sCMOS Neo cameras as a function of the wavelength. The emission ranges of several fluorophores are included for reference. Taken from the Andor Neo sCMOS hardware guide [19].

a PBS cage, which is mounted to the table using another post holder. This means that we can adjust both the height and the horizontal angle of the cage, while the other parameters are fixed. Because of the tubing however, the rotation and height will automatically be fixed to some extent. The PBS-cage allows for fine adjustment of the orientation of the PBS-cube (in all 3 directions), after the cage has been fixed. This is used in manually making sure that the images on both cameras overlap.

3.4 Consequences of the setup

The elements of the setup are not perfect, so we will have some anisotropy affecting factors which were not covered in the theory section. In this section we will describe these factors, how they affect the anisotropy and how to deal with them.

3.4.1 Background and thermal noise

Any camera reads a certain amount of background. This background can be split into two parts: fundamental and non-fundamental. The fundamental background of the cameras is the signal we get when no photons hit the chip. This background also contains so called "hot pixels". These are pixels which have a high count because they have been triggered by random thermal energy. To combat these hot pixels, the chip can be cooled down to -40°C , and the imaging software can automatically removes single-pixel spikes in the image (spurious noise filter). The non-fundamental background is the part of the background which is caused by light from the environment, light which is reflected by the sample but

not filtered out by the dichroic cube, and light from fluorescence of other components of our sample. We can account for all background, by performing a measurement on a sample with only solvent. We can then subtract this from our measurements with the real samples. All that remains then (in principle) is the noise band of the background, which can be measured as well and must be considered in calculating the final uncertainty in the measurements. Obviously in all of these measurements (of the background and of the samples), all other light sources must be shut off to reduce background and to make the background consistent.

3.4.2 G-factor

Our setup contains many optical components which have a different effect on parallelly and perpendicularly polarized light. In some of the components this is supposed to happen (like in the polarizing beam splitter and linear polarizers), but in many it isn't (like in the mirrors, the objective, and the lenses). The net effect of all the components is that parallel and perpendicular light will not be treated equally, yielding a nonzero anisotropy even for perfectly anisotropic light. To combat this, we must know by what factor parallel light is preferred over perpendicular by the setup. This factor is called G , and its value can be different for every pixel of our image. Once it is determined we can compensate for the preferential treatment of our setup by calculating the anisotropy as follows:

$$r = \frac{I_{\parallel} - GI_{\perp}}{I_{\parallel} + 2GI_{\perp}} \quad (30)$$

How do we determine G ? We need a source of completely isotropic light. If the setup were perfect, we would read equal values of I_{\parallel} and I_{\perp} . In our actual setup I_{\parallel} is treated preferentially by a factor of G , so then $I_{\parallel} = GI_{\perp}$, or:

$$G = \frac{I_{\parallel}}{I_{\perp}} \quad (31)$$

We stress again that G is different for every pixel, so G is an image, not a single number. How to produce a perfectly anisotropic source of light will be explained in section 4.2.

3.4.3 Misaligned images

Since the setup must be aligned by hand, and the size of a pixel is only 6.5 microns, it is not possible to align both cameras perfectly. Therefore, an object on camera one will appear in a slightly different place on camera two. Besides translation we may also have some rotation, magnification and shear. The images must therefore be aligned by use of software. For this purpose we define a transformation matrix T which determines the transformation between camera one and camera two. T is represented by a 3x3 matrix with the following entries:

$$T = \begin{pmatrix} A & B & 0 \\ C & D & 0 \\ X & Y & 1 \end{pmatrix} \quad (32)$$

The location of a pixel on either camera one or two is represented by a 1x3 row vector, whose first two entries are the horizontal and vertical positions of the pixel, and whose last entry is 1, e.g. $(x, y, 1)$ for pixel (x, y) . This allows us to have translations (this is not possible with a 2x2 matrix and 2x1 vectors). We say that the image from camera one is the stationary image, and we must transform the image from camera two onto it. Therefore, if we have a pixel on camera two specified by $\vec{v}_2 = (x_2, y_2, 1)$, we must apply T to it to get $\vec{v}_1 = (x_1, y_1, 1)$:

$$\vec{v}_1 = (x_1 \quad y_1 \quad 1) = \vec{v}_2 T = (x_2 \quad y_2 \quad 1) \begin{pmatrix} A & B & 0 \\ C & D & 0 \\ X & Y & 1 \end{pmatrix} = (x_2 \quad y_2 \quad 1) \begin{pmatrix} A & B & 0 \\ C & D & 0 \\ 0 & 0 & 1 \end{pmatrix} + (X \quad Y \quad 0) \quad (33)$$

Now we recognize the X and Y entries of T as the translation part, and we see that the ABCD-block determines the rotation, magnification and skew. The matrix T can be determined by imaging the same sample on both cameras, and subsequently letting a computer program optimize T until the difference between image one and T applied to image two is minimal. More about this in sections 4.1 and 5.

3.4.4 Numerical aperture

Another important factor in our setup is the numerical aperture NA of our objective. The numerical aperture specifies the range of angles under which our objective can accept light from the environment. It is defined as follows:

$$NA = n \sin(\sigma) \quad (34)$$

Where n is the refractive index of the medium the objective is immersed in, and σ is the largest possible half-angle under which the objective can receive light (see figure 6). The refractive index n is included in the definition to account for the immersion medium of the objective. This can be seen by imagining another medium with a flat interface, halfway through figure 6. Now, using Snellius' law it can easily be seen that $\sin(\sigma)$ changes by a factor of n across the interface. Since we will only be using air as a medium, $n = 1$ and NA is simply $\sin(\sigma)$.

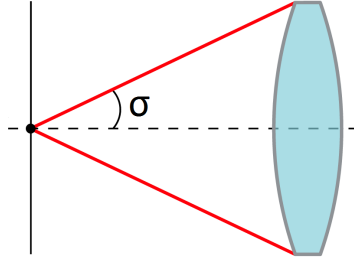


Figure 6: A graphical representation of the half-angle σ , which specifies the largest angle under which the objective can receive light.

Now, the numerical aperture of our objective is relevant for several reasons. The first is the most obvious: a larger numerical aperture means a larger angle under which light can be collected, which means that we get more signal. The second reason is that the numerical aperture affects the resolving power of the objective. The size of the smallest features that can be resolved is proportional to $\lambda/2NA$, where λ is the wavelength of the light used. Furthermore, the depth of field also decreases with increasing NA , so the depth resolution is also improved. So far it seems that the higher the numerical aperture, the better. However, there is a catch. The lens of the objective affects the polarization of the light emitted by the fluorophores, which skews our anisotropy measurements. This effect is stronger for a larger numerical aperture. In order to quantify this effect we need to define a righthanded coordinate system with axes X_1 , X_2 , and X_3 , where X_1 runs parallel to the optical axis of the objective, and X_3 is parallel to the excitation polarization. The origin will be a static fluorophore in the sample, with an orientation given by a unit vector (x_1, x_2, x_3) . Now, for a given orientation of the fluorophore and a given σ , the measured parallel and perpendicular intensities (I_{\parallel} and I_{\perp}) turn out to be [17]:

$$\begin{aligned} I_{\parallel} &= K_a x_1^2 + K_b x_2^2 + K_c x_3^2 \\ I_{\perp} &= K_a x_1^2 + K_c x_2^2 + K_b x_3^2 \end{aligned} \quad (35)$$

with:

$$\begin{aligned}
K_a &= \frac{1}{3}(2 - 3\cos(\sigma) + \cos^3(\sigma)) \\
K_b &= \frac{1}{12}(1 - 3\cos(\sigma) + 3\cos^2(\sigma) - \cos^3(\sigma)) \\
K_c &= \frac{1}{4}(5 - 3\cos(\sigma) - \cos^2(\sigma) - \cos^3(\sigma))
\end{aligned} \tag{36}$$

Using this we can now (numerically) calculate the expected anisotropy for a static, isotropic distribution of fluorophores, as a function of σ . The result of this can be seen in figure 7.



Figure 7: The anisotropy of a static, isotropic distribution of fluorophores, with the NA-effect. r is the anisotropy and σ is the aperture half-angle in degrees.

We see that when our numerical aperture gets larger, σ gets larger and our anisotropy is lowered. Therefore, in choosing a numerical aperture we have a competition between resolution and intensity, and unskewed polarization. We believe that our $NA = 0.6$ objective strikes a reasonable balance between the two. The maximum half-angle for our objective is $\sigma \approx 37^\circ$, which means that the anisotropy is lowered by about 6%.

3.5 Autofluorescence

Cells contain many different kinds of proteins, some of which may fluoresce in the part of the spectrum we're measuring. This is called autofluorescence and is an important factor in calculating the anisotropy. When we measure the parallel and perpendicular fluorescence intensities from our labeling protein, we are also going to get autofluorescence in our signal. This autofluorescence can be isotropic or anisotropic, depending on the proteins causing it. To get the true anisotropy of our labeling protein, we must subtract the autofluorescence from our images. We can split up the autofluorescence into a parallel A_{\parallel} and perpendicular part A_{\perp} , so that the net anisotropy becomes:

$$r = \frac{(I_{\parallel} - A_{\parallel}) - G(I_{\perp} - A_{\perp})}{(I_{\parallel} - A_{\parallel}) + 2G(I_{\perp} - A_{\perp})} \tag{37}$$

To see the effect of autofluorescence on our measurements, assume that $G = 1$, and say that the net parallel and perpendicular intensities of our labeling cell are 8000 and 4500, so our anisotropy is 0.3. Now assume that we have some autofluorescence A_{\parallel} and A_{\perp} , which we don't subtract from our measurements. The effect on the anisotropy can be seen in figure 8 for different values of A_{\parallel} and A_{\perp} .

We can see that the effect of incorrect autofluorescence subtraction is quite large. This is relevant because it is actually very hard to determine and subtract the autofluorescence. First of all, the autofluorescence

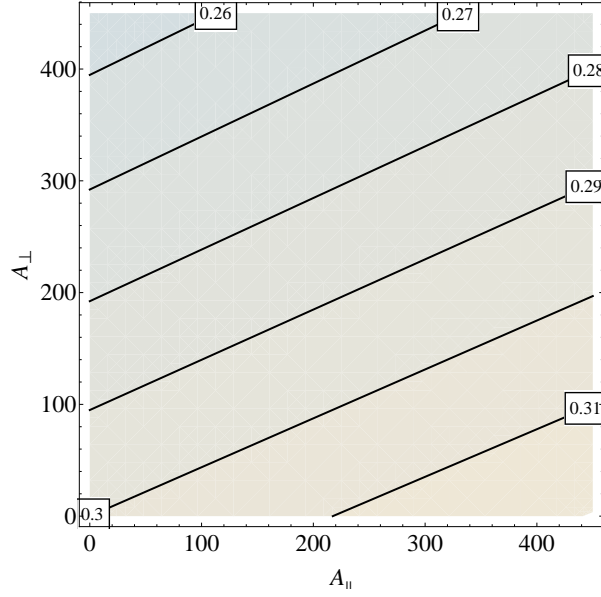


Figure 8: The effect of autofluorescence on anisotropy. The black lines are contours of equal anisotropy.

varies greatly within a cell. Different components like the nucleus, the cytoplasm and the membrane can have different values of $A_{||}$ and A_{\perp} . Furthermore, the autofluorescence varies between cells. Large cells tend to be brighter than smaller cells, but even cells of the same size have varying autofluorescences. Since we can't measure the autofluorescence of a labeled cell, we must measure it in unlabeled cells *of similar size and brightness* to the cells we want to study. By this we mean that in both labeled and unlabeled samples we look for cells of approximately average size and brightness, so that we measure "typical cells" in both cases. This gives a significant amount of uncertainty in the autofluorescence, which is why we decided to measure in the red part of the spectrum. Theoretically, the autofluorescence of cells is lower in the red part of the spectrum, and so the uncertainty in the autofluorescence will have less of an effect on the final autofluorescence calculation.

3.5.1 Combining autofluorescence and background

Since background is subtracted in the same way as the autofluorescence, we measure both as a single combined value. There is no real point in subtracting the background from the autofluorescence to gain the "true" autofluorescence, since we need to subtract them both from our images anyway.

4 The measurement process

4.1 Image beads

First we image a set of 200nm yellow-green fluorescent beads, in order to determine the alignment of our cameras. Since they fluoresce yellow-green, we must use dichroic A in order to be able to image them properly. Note that this doesn't mean that the setup will now be aligned only for the green dichroic. Reference measurements have shown that the difference in alignment for the green and the red part of the spectrum is negligible. Nonetheless we do recommend using red fluorescent beads or something similar for future experiments (simply because it is more consistent). For the sake of intensity, we don't use the excitation polarization filter (there is no point exciting the beads with polarized light). Since each pixel represents about 160nm, the beads should be about 2x2 pixels each. Actually they show up as blobs of around 10x10 pixels with radially decreasing intensity, which signifies significant diffraction effects. This is not surprising, as our imaging wavelength is larger than the beads themselves. Depending on the focus, we can also see Airy diffraction rings. For alignment purposes we decided to image the beads when the rings are least visible (so slightly out of focus). The first part of alignment is done physically, by moving the PBS-cube by hand until the images roughly overlap. With this we can already get the images to within about 10 pixels of each other. We then fix the orientation of the PBS cube by tightening the screws and image the beads with both cameras. The last part of alignment will be determining the T-matrix from these images, which will be discussed further in section 5. To make sure the alignment script can determine the T-matrix properly, we must make sure that there are no beads on the edges of our images (this might confuse the optimization algorithm).

4.2 Image rhodamine

Next, we need to determine the G-factor of the setup. To do this, as we discussed earlier, we need a perfectly isotropic source of fluorescence. Simply imaging without an excitation filter is not enough, as there are other elements in the excitation path which can alter the polarization of the light. To compensate for this, we image a solution of rhodamine-B in water. Rhodamine-B is a small fluorophore, so it rotates quickly. As can be seen in table 1, the rotational correlation time of rhodamine-B in water is much smaller than its fluorescence lifetime. Therefore, we expect the emission to be fully depolarized, so the light coming from the sample should be perfectly isotropic. In our sample we use a 5 μM solution of rhodamine-B, since this gives us sufficient intensity. The solution is sandwiched between a standard glass microscopy slide and a glass coverslip. The glass slide has been pre-treated (washed twice) with bovine serum albumin (BSA). This makes sure that the rhodamine doesn't adsorb to the slide, since the adsorption places are already taken by the BSA. We do this because there has been trouble in the past with proteins adhering to the glass [1]. BSA is commonly used as a generic protein, and its emission spectrum is in the near-UV, so it won't interfere with our measurements. In short we image our sample of rhodamine-B without an excitation filter, and obviously using dichroic C. To accurately determine G, we must also determine the background. To do this, we image a sample containing only water and BSA under the same conditions. We get the net rhodamine signal by subtracting these images from the rhodamine-images.

4.3 Image mCherry

Now we need to determine the maximum anisotropy we can get with the setup. To do this we image a sample of mCherry in glycerol, *with* excitation polarizer filter (otherwise we couldn't measure anisotropy), and of course with dichroic C. Since mCherry is a large molecule and glycerol has a high viscosity, the rotational correlation time will be high. Since the rotational correlation time is much higher than the fluorescence lifetime, rotational diffusion will have no effect on the anisotropy. Therefore we would expect an anisotropy close to 0.4, barring the effects of numerical aperture and non-parallel excitation/emission axes. In our sample we use a 5 μM solution of mCherry in glycerol, which also contains 8mg/ml BSA to combat adsorption. In addition, the coverslip has been pre-treated with BSA as well. So we image the mCherry sample. We also image a sample containing only glycerol, which has been prepared in the same way, to measure background.

4.4 Image unlabeled cells

The next step is measuring the autofluorescence. For this we use endothelial cells, which is the same type of cell we will be labeling for homo-FRET. The cells are incubated and subsequently sown onto a microscope slide and fixed in polyvinyl alcohol. To measure the autofluorescence consistently, we select cells which look healthy (they aren't shriveled up), and which are of average size and intensity. Also, we put the cells in the same spot (on the camera) every time, so we don't get inconsistencies caused by darker or lighter parts of the chip. We image with dichroic C, and with polarization excitation filter (since we will be using these for the labeled cells as well). We need to image at least 10 cells to get an idea of the average autofluorescence. Later we split up the autofluorescence into three parts: The nucleus, the cytoplasm, and the membrane. More about this in section 5.

4.5 Image labeled cells of interest

The last step is to measure the labeled cells, in the same way as the unlabeled cells (same filters and same imaging time). We use endothelial cells, whose DNA has been spliced with the gene that encodes for mCherry. These cells are incubated and sown just as the unlabeled cells. We use two different types of mCherry-producing cells. The first type produces mCherry-FKBP. FKBP is a protein which is known to cluster when exposed to AP, so we should be able to measure anisotropy decrease between cells with and without AP. Therefore, we image mCherry-FKBP cells with and without added FKBP. The second kind of cell produces mCherry-FKBP-EGFR. EGFR (epidermal growth factor receptor), is a protein which is found mostly on the membrane of a cell, and which regulates cell growth. It is activated by EGF (epidermal growth factor), and it is expected to cluster [16]. We can check this clustering by measuring the cells with this protein-construct, both with and without EGF. We can also measure the cells with AP, to make sure the construct can cluster (it might be too large or something different might be going on). In all measurements we must make sure that we use the same imaging-time and that we put the cells in the same place as the unlabeled cells (for consistency).

5 Data analysis

In this section we discuss how to analyze our data. We use *MATLAB* and *ImageJ*. A collection of the *MATLAB* scripts used can be found in section 10.

5.1 Determining T

The first step is to determine the T-matrix. For this we need to first import the bead-images from both cameras into the workspace. Now the `alim` function can be used to determine the T-matrix as follows:

```
T = alim(im1, im2, Tstart);
```

Here `im1` is the bead image from camera one and `im2` is the bead image from camera two. The third argument is optional and we will discuss it in a moment. The function uses a mutual information metric to iteratively optimize the transformation matrix between the images. It starts out with an identity matrix and tries out small changes. When a change improves the metric, it is kept and new changes are tried. When the matrix can not be optimized further or after a maximum of 500 iterations, the iterative process stops and the matrix is saved in the workspace under the name `T`. At the same time, a figure is created which shows how well the images were made to overlap by `T`. The image from camera one is shown in green, and the transformed image from camera 2 is shown over it, in red. When the images overlap perfectly everything should be white and there should be no green or red edges to the beads. The T-matrix can also be checked manually by simply opening it in the workspace, keeping in mind that the first 2x2 block is a 2x2 transformation matrix, and the last two entries signify a translation. Sometimes the function does not produce a good transformation matrix, because the optimizer got stuck in a local minimum or because the alignment between the images was too poor to start with. To get a good transformation matrix we must therefore specify a better starting matrix. A starting matrix can be created manually by editing `T` in the workspace, and seeing how well it works using the `imshowpair` command:

```
imshowpair(im1, imwarp(im2, T, 'OutputView', imref2d(size(im1))))
```

This creates a red-green overlap image, just like the one the function outputs. We must manually alter `T` until the overlap is "reasonable". We can then use `T` as the starting matrix for our optimization, by using it as the third argument in the `alim` function. This will almost always yield a good matrix. If the third argument is left blank, the starting matrix will simply be the identity matrix.

5.2 Determining G

First open the images of the blanc rhodamine sample in *ImageJ*, and determine their average intensity. This gives us the background values of camera one and two. Determining the G-image is simple. Import the rhodamine images from both cameras into the workspace. Then use the `calg` function:

```
G = calg(im1, im2, T);
```

Here `im1` and `im2` are the rhodamine images from cameras one and two, and `T` is the transformation matrix determined in the previous section. If we want to take background into account, we can subtract our background values from both `im1` and `im2` before using them in `alim`. The `alim` function simply applies the T-matrix to `im2`, and divides `im1` by this result on a pixel by pixel basis. If `T` is left blank, it will use the identity matrix. After `im2` has been transformed, there are some areas in `im1` where `im2` does not exist. This causes extremely high G-values near the edges of these areas, and infinities within these areas. Therefore `alim` turns all G-values higher than 1.45 into zero. Finally, the G-image is saved in the workspace under the name `G` and a new figure is created which shows the G-image. After `G` has been determined, we can also calculate the average G-value as follows:

```
mean(nonzeros(G))
```


5.3 Determining the maximum anisotropy

First open the images of the blanc mCherry sample in *ImageJ*, and determine their average intensity. This gives us the background values of cameras one and two. Now import the mCherry images from both cameras into the workspace. We can now calculate the maximum anisotropy by using the **anis** function:

```
ani = anis(im1, im2, G, T, auto1, auto2);
```

Here **im1** and **im2** are the mCherry images from cameras one and two, **G** is the G-factor image, **T** is the transformation matrix, and **auto1** and **auto2** are the backgrounds of the blanc mCherry-samples for cameras one and two. The function transforms **im2** according to **T**, and subtracts **auto1** and **auto2** from both **im1** and the transformed **im2**. Then it uses **G** to calculate the anisotropy image using equation 37. Infinities are automatically changed to zero. The anisotropy image is saved in the workspace under the name **ani**, and a new figure is created which shows the anisotropy image. The average anisotropy can be calculated as follows:

```
mean(nonzeros(ani))
```

Note that the **ani** function can also be used to determine the anisotropy of any other pair of images with constant backgrounds.

5.4 Determining the autofluorescence

First open the blanc cell images in *imageJ*. Now using the freehand selection tool we can select regions, and measure the average intensity in these regions. Now there are two ways to handle the autofluorescence. The simplest way is to measure average intensities of whole cells. Averaging over all the cells we measured, we get just two values: the parallel and the perpendicular autofluorescence. These constant values will then be subtracted from the labeled cell images before calculating the anisotropy of the labeled cells. This method is simple, but it ignores the fact that the autofluorescence of cells is different in different areas of the cell. The second method is to split the cells up in different regions, like membrane, cytoplasm, and nucleus. For each blanc cell, the average autofluorescence can be measured for each region. Averaging over all cells, we then get (in this example with three regions) six different values: The parallel and perpendicular autofluorescence intensities for all three regions. To subtract these values from the labeled cell images, the regions must be manually specified in the labeled cell regions as well. This takes a lot of time and will be explained later. Apart from the fact that this method takes more time, it also might not be possible at all since it can be very hard to distinguish different cell-features in autofluorescence images, since they are very dim.

5.5 Determining the anisotropies

As mentioned earlier, there are two ways to handle autofluorescence. In the actual analysis, they are handled the same way. First make sure the images of the labeled cells are split up into two folders called **CAM1** and **CAM2**, which are in the same directory. For each folder the cells should be labeled by only a number. Write down what kind of cell each number is somewhere else. Now open up the parallel image of each cell, and select the whole cell, using either the freehand select or threshold select tool (ctrl-shift-T). Now we need to turn this selection into a so called mask, by going to **edit>selection>create mask**. This is basically a binary image which specifies a region of interest. Save the mask as **imj.tif** in some designated folder, where **i** is the number of the cell, and **j** specifies which mask it is. For whole-cell autofluorescence, each cell only has one mask and so we get **1m1.tif**, **2m1.tif**, **3m1.tif** etc. When we use split autofluorescence, we need to create multiple masks for each cell. These should be nested. For example when we our regions are membrane, cytoplasm, and nucleus, our first mask would be the entire cell, the second would be the entire cell minus the membrane, and the third would be just the nucleus. We would save these as **1m1.tif**, **1m2.tif**, and **1m3.tif** (for cell 1). Once we have created masks for all our cells we are done with *imageJ*, and we can start using them in *MATLAB*. First, we create a collection of regions of interests using the **roifrommask** function:

```
roi = roifrommask(link, imnum, propnum, inverted);
```

Here `link` is the directory of the masks (as a string ending in a backslash), `imnum` is the number of cells that were imaged, `propnum` is the number of masks for each cell, and `inverted` is either 0 or 1 and determines whether or not all the masks should be inverted before processing (toggle this if the ROIs turn out wrong). The `roifrommask` function uses the nested masks to create logical ROI (region of interest) images which are no longer nested. In our membrane-cytoplasm-nucleus example, for each cell the function would create a ROI-image which specifies the membrane, the cytoplasm, and the nucleus, with no overlap. It does this for every cell, so in the end we get a whole cell (array) of ROIs, which is saved in the workspace under the name `roi`. A cell is a type of array *MATLAB* uses, which is different from a standard "array" array. This might be a bit confusing since cells are also what we image, but it should be clear which kind of cell is meant from the context. The ROIs can be individually checked for errors if needed, for example `roi{9,3}` gives the third region of interest for cell 9. Now we need to create a cell of the autofluorescence values we found in the previous section. For example in our membrane-cytoplasm-nucleus example, an autofluorescence cell could look like this:

```
auto={400,200 ; 300,150 ; 500,250};
```

Here 400 and 200 would be the average parallel and perpendicular autofluorescences of the membrane, 300 and 150 would be the average parallel and perpendicular autofluorescences of the cytoplasm, etc. For whole-cell autofluorescence our autofluorescence cell would only have two entries: the average whole-cell parallel and perpendicular autofluorescences. Now we are finally ready to calculate anisotropies. This is done using the `process3` function. Note that the 3 just means that it is the third version of the process function, it has nothing to do with the amount of masks per cell. All functions are made so that they work for any number of masks per cell, including only one. The `process3` function is used like this:

```
[x, a] = process3(link, G, T, roi, auto)
```

Here `link` is the directory both CAM-folders are in. This should be input as a string, ending in a backslash. Furthermore `G` and `T` are the G-image and T-matrix, `roi` is the ROI-cell, and `auto` is the autofluorescence cell. The `process3` function automatically loads all the images into the workspace, as one cell entity `x`. The first coordinate of `x` signifies the cell number and the second whether it is the image from camera one or two. For example `x{7,2}` is cell 7 as imaged by camera 2. The function subsequently calculates the anisotropy images of all the cells, using the different autofluorescence values in the different regions of interest. Again, infinities are automatically changed to zero, and the anisotropy images are saved in the workspace as a cell called `a`. This cell only has one dimension, since there is only one anisotropy image per cell. Finally, all the anisotropy images are shown on screen in separate figures. After checking these for errors, we can calculate the average anisotropy for each region of interest and each cell, by using the `avanis` function:

```
ava = avanis(a, roi);
```

This function creates a cell called `ava` in the workspace which contains all these averages. For example, `ava{11,3}` would be the average anisotropy in the third region of interest (probably nucleus) of the eleventh cell.

5.6 Saving the data

Firstly the anisotropy data can be saved using the `savanis` function:

```
savanis(a, place, name);
```

Here `a` is the cell of anisotropy images, `place` is the directory where the anisotropy data is placed (as a string, ending in a backslash), and `name` is the name that will be put in front of each file. The function

turns every anisotropy image into a figure with a colorbar, and saves these figures as eps files, which can be included in for example \LaTeX documents. It also saves the anisotropy images multiplied by 1000 as tif files in the same directory, so they can be further inspected using *ImageJ* if needed. The average anisotropies can be saved by simply double-clicking the **ava** cell in the workspace and copying the data to a spreadsheet or something similar. This can also be done for the T-matrix. All other images can be saved by showing them in a figure using the **imshow** command, and subsequently saving them as an eps file. Note that adding **af;** or **ggf;** after an **imshow** statement adds parameters (such as a colorbar) which are suited for anisotropy and G-value images respectively. Lastly, the workspace as a whole can be saved to continue data analysis at a later time.

6 Uncertainty

There are many sources of uncertainty in our experiment. Some of these are systematic, and some are random. The most important sources of systematic uncertainty are:

- The anisotropy lowering effect of the objective
- Small misalignment of the cameras

These are uncertainties we can't do much about. The anisotropy lowering effect of the objective can be roughly estimated from the theory of high NA anisotropy lowering, and can be checked to some extent by measuring the maximum anisotropy. Any misalignment of the cameras which can not be noticed must be smaller than about one pixel. This degree of misalignment can certainly affect the anisotropy of a single pixel, but probably won't affect the average anisotropy of a larger area much. The most important sources of random uncertainty are:

- Uncertainty in the G-factor
- Uncertainty in the autofluorescence values
- Photon statistics

The uncertainty in the G-factor and autofluorescence values can be estimated from reference measurements, and photon statistics uncertainties can be approximated using the method described in section 6.1. Since we have one equation which contains all the variables corresponding to these uncertainties (equation 37), we can apply differential propagation of uncertainty to estimate the final uncertainty in the anisotropy r :

$$\delta_r = \sqrt{\left(\frac{\partial r}{\partial I_{\parallel}} \delta_{I_{\parallel}}\right)^2 + \left(\frac{\partial r}{\partial I_{\perp}} \delta_{I_{\perp}}\right)^2 + \left(\frac{\partial r}{\partial A_{\parallel}} \delta_{A_{\parallel}}\right)^2 + \left(\frac{\partial r}{\partial A_{\perp}} \delta_{A_{\perp}}\right)^2 + \left(\frac{\partial r}{\partial G} \delta_G\right)^2} \quad (38)$$

Here r is the anisotropy, I_{\parallel} and I_{\perp} are the measured parallel and perpendicular intensities, A_{\parallel} and A_{\perp} are the estimated parallel and perpendicular autofluorescence values, and G is the G-value. Furthermore, a δ indicates the uncertainty in a variable. This method can be applied to calculate the uncertainty in a single pixel, or to calculate the uncertainty of the average anisotropy in an area.

6.1 Photon statistics uncertainty

In theory the stream of photons that hit the chip obey Poisson statistics, so the standard deviation of the number of photons that hit a pixel is equal to the square root of the average amount of photons that hit that pixel (in a certain time). However, it is possible that one photon leads to multiple counts in the final image, so that we can't use the same square root trick directly for our measured counts. Let's say that we expect N photons to hit a pixel, so that the standard deviation is \sqrt{N} . Say that for every photon we get α counts in our image. Then the expected amount of counts will be αN with a standard deviation of $\alpha \sqrt{N}$. If we applied the square root trick directly to the amount of counts, we would instead expect a standard deviation of $\sqrt{\alpha} \sqrt{N}$. Therefore the standard deviation in our counts will always be a constant factor $\sqrt{\alpha}$ greater than the square root of our amount of counts. We can determine $\sqrt{\alpha}$ by measuring the average and standard deviation of a homogenous image with a high amount of counts per pixel.

7 Reference measurements

7.1 Background

We measured the background reading in both cameras (completely shielded and disconnected from the microscope), at different chip temperatures and with/without environmental light. All tests were carried out with the rolling imaging setting, with an imaging time of 10 seconds. For the tests with environmental light, we turned on all the lights in the lab (including intense overhead lamps). For the tests without environmental light, we turned off all light sources with the exception of some LED's of devices that could not be turned off. The results of the measurements can be seen in table 3.

Camera 1	Lights on	Lights off
-15C°	182/15	101/2.3
-35C°	178/15	101/2.3
Camera 2	Lights on	Lights off
-15C°	105/3.0	101/2.2
-35C°	105/2.9	101/2.1

Table 3: The background reading in both cameras at different chip temperatures and with and without environmental light. Every entry is the average measured value over the entire chip, followed by the standard deviation over the entire chip.

We see that the fundamental (readout) background seems to be about 101 counts on both cameras. This is independent of measuring time, as we will see later. Furthermore we see that having environmental light can have a significant impact on our reading, even when a camera seems to be completely shielded (as was the case with both cameras). Therefore in all later measurements we turned off all environmental light. Lastly, the temperature doesn't seem to influence either the average number of counts or the standard deviation. However, setting the chip temperature lower does reduce the amount of hot pixels. This can be seen quantitatively because the largest number of counts for a pixel was consistently significantly lower when the chip temperature was -35C° instead of -15C°.

7.2 Photon statistics

We measured the average and standard deviation of a homogenous part of an image of fluorescein. The image was made using the rolling imaging setting, and had an exposure time of three seconds. In a homogenous looking area of 2200 pixels we found an average amount of counts of 32300 and a standard deviation of 231. This would indicate that $\sqrt{\alpha}$ is about 1.3.

7.3 Comparison of rolling and global measurement

We measured the background in both cameras for different exposure times using both the rolling and the global shutter setting. The results can be seen in table 4

Time (in seconds)	Global	Rolling
.05	102/102	101/101
.1	102/102	101/101
1	102/102	101/101
10	102/102	103/102
30	105/102	108/103

Table 4: The background reading in both cameras at different exposure times and using the global or rolling setting. Each entry contains the average number of counts in both cameras, separated by a forward slash.

We see that there is no difference in the fundamental background between global and rolling shutter. We also see that the fundamental background is mostly independent of exposure time, rising slightly only at very high exposure times. The noise band in the fundamental background signal was on the order of 2-10 counts for both rolling and global shutter mode. The contribution of the noise band of the fundamental background is therefore negligible in the final anisotropy uncertainty calculation. During other measurements with fluorescein we noticed that in rolling shutter mode we always get roughly three times as many counts as in global shutter mode. However, the standard deviation is also three times as high, so we don't actually get a higher degree of accuracy by using the rolling shutter mode. However, since the fundamental backgrounds in both rolling and global shutter mode are equal, the fundamental background is relatively less intense in rolling shutter mode. Therefore, we decided to use rolling shutter mode in most future measurements, although there is really not much of a difference. We also noticed that when the number of counts gets too high, we get a strange splitting effect in our image. This effect causes one half of the image to be significantly less bright than the other half, and distortion lines appear (see figure 9). In global shutter mode this occurs around 13000 counts per pixel, while in rolling shutter mode this occurs around 40000 counts per pixel (this is at the same light intensity since rolling shutter gives three times as many counts). When the number of counts goes even higher, the entire image will just show a constant reading of 53000. Obviously to get good images we must stay below these values.

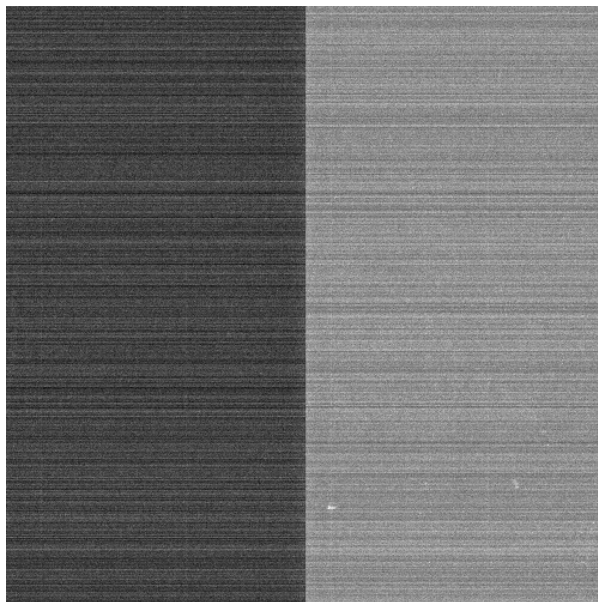


Figure 9: The splitting effect when the number of counts gets too high. This image is of a fluorescein sample, measured using the global shutter mode with an exposure time of 10 seconds. The average number of counts on the left side of the image is about 17000, and on the right side 18000. Also note the horizontal lines of varying intensity.

7.4 Explanation for all camera aberrations

Upon further examination of the camera manual [19], we found that the cameras have two possible gain factors for 16-bit imaging. The gain factor is either 0.6 or 1.6. This means that every electron-hole pair leads to either 0.6 or 1.6 counts. We suspect that the rolling shutter mode automatically uses a gain factor of 1.6 counts, while the global shutter uses a gain factor of about 0.6. In rolling shutter mode we would therefore expect about 2.5 times as many counts. This is not exactly equal to the factor of three we have seen in other reference measurements, but the manual says the gain factors are "typical", so there might be some deviation from the reported values. We suspect that the gain factor in rolling shutter mode is actually closer to 1.7 or 1.8. This would also explain the value of 1.3 for $\sqrt{\alpha}$ we found, since $1.3^2 \approx 1.7$. Finally, the difference in gain factors between rolling and global shutter mode also explains why the electron saturation level (which causes the splitting effect) is reached three times as

early in global shutter mode.

7.5 Intensity comparison of dichroic cubes A, B and C

We measured the intensity of the excitation light at the sample location using dichroic cubes A, B and C. We found the intensity at the specimen for dichroic cube A to be 0.14 mW, for B to be 0.37 mW, and for dichroic C to be 0.78 mW. Compensating for the fact that light intensity is inversely proportional to the wavelength, we find the relative photon fluxes using dichroics A, B and C to be about 14, 40 and 87. We see that using dichroic B our sample is illuminated about thrice as much, and using dichroic C about six times as much as with dichroic A. This makes sense when we look at the emission spectrum of mercury. The excitation filter in dichroic B lets through a major peak in the spectrum, and dichroic C lets through two peaks, while no significant peaks are present in the excitation filter range of dichroic A. This excitation intensity difference is relevant when we compare backgrounds and autofluorescences for the different dichroics.

7.6 Factors in the environmental background

We measured several types of background using dichroic A and B. First we measured the effect of scattering in the environment. We turned on the mercury lamp and used the polarization excitation filter, so the objective emits excitation light. We used no sample, so the objective is free to collect scattered reflections and other light from the environment (sporadic LEDs that could not be turned off). We did this with dichroic cubes A and B, with and without a rubber cap over the sample area, and with an exposure time of one and ten seconds, using the global imaging setting. The results of this can be seen below in table 5.

Without rubber cap:	Time (in s)	Dichroic A	Dichroic B
	1	105/102	107/104
	10	149/108	165/132
With rubber cap:	Time (in s)	Dichroic A	Dichroic B
	1	106/102	107/104
	10	152/109	172/134

Table 5: Measurements of the background caused by scattering in the environment, measured with both dichroic A and dichroic B, and both with and without a shielding rubber cap over the sample area. Each entry contains the average number of counts in the image, for both camera one and two, separated by a forward slash.

First of all we see that the effect of environmental light is rather small, being comparable to the fundamental background only when the imaging time is ten seconds. We see that the environmental background is slightly more intense for dichroic B. However, considering the fact that the excitation light from dichroic B is three times as intense as from dichroic A, and the fact that the cameras are slightly more sensitive to red light than to green light, this means that the scattered light is actually relatively less intense for dichroic B. Interestingly, putting a shielding rubber cap over the sampling area, which is supposed to stop environmental background, makes the background slightly more intense. This is probably because the cap itself scatters the excitation light more efficiently than the environment. We get about the same number of counts when we replace the entire objective by a stopping cap, indicating that it truly is scattering that contributes most to this background. We also performed measurements in the same way as above, with empty samples (just microscope slides) and with samples of polyvinyl alcohol. With an exposure time of ten seconds, we found the intensity in the green to be 184/129 and in the red to be 286/207 for an empty sample. For a sample of polyvinyl alcohol the intensities were 209/139 in the green and 371/250 in the red. This shows that the base of our samples contributes slightly to the background, although all in all it still is a pretty small amount.

7.7 Intensity comparison of Rhodamine-B, Fluorescein, mCherry and GFP

We measured the intensities of rhodamine-B, fluorescein, mCherry and GFP, using dichroic A for the green fluorophores and dichroic C for the red fluorophores, and using camera one. The results of this can be seen in table 6.

Fluorophore	Concentration(in μM)	Time (in s)	Counts	Rel. Int.
Rhodamine-B	5	0.2	23200	23200
Fluorescein	31	5	27500	177
mCherry	5	0.2	32400	32400
GFP	3.5	5	10600	605

Table 6: The average amount of counts for different fluorophores. Also included is the relative intensity (Rel. Int.), which is calculated by dividing the average number of counts by the concentration and the exposure time. Note that this does not reflect the actual brightness of the fluorophores, it is merely a comparison of what intensities we can expect from the various fluorophores using our setup with dichroics A and C.

We see that the relative intensities of rhodamine-B and mCherry are much higher than those of fluorescein and GFP. This can partly be explained by the fact that our excitation beam is more powerful in the red part of the spectrum, that the camera is slightly more sensitive to red light, and the fact that dichroic cube C has a broader emission bandfilter. Also, dichroic A was not perfectly suited for use with GFP, since the emission maximum of GFP falls outside of its emission band filter range. Still, a factor of over 100 between the intensities of rhodamine-B and fluorescein seems extremely high. We must note that the fluorescein and GFP samples were several months old. However, when we measured the intensities of GFP and fluorescein several months earlier, they were about the same. Furthermore, in his thesis [1], Nivard Kagie mentions using 10 second imaging times for his reference measurements on 3.5 μM GFP solutions. This means he couldn't have gotten more than about 40000 counts, because he would have gotten the splitting effect and his measurements would have been invalid. His fluorescein measurements seem to match our intensity results as well. We conclude that rhodamine-B gives us about 130 times as many counts as fluorescein, and that mCherry gives us about 50 times as many counts as GFP.

7.8 Camera alignment with different dichroic cubes

We wanted to know if using a different dichroic cube would significantly change the alignment of our cameras. Since our alignment beads only fluoresce in the green part of the spectrum, we used three different green dichroics, with different excitation and emission wavelengths. One of these was dichroic A. We imaged a set of 200nm green fluorescent beads with the three dichroics, and determined the transformation matrix T for each of them. The differences between the matrices were on the order of 1/10000 for the A, B, C and D values and on the order of 0.1 for the X and Y values. This indicates a difference of about 0.1 pixels in the alignment, which is negligible. We therefore estimated that the difference in alignment between dichroics A and B or C would not be very large either, so we could continue using dichroic A for alignment.

7.9 G-factor measurements with dichroic B

We measured the G-factor of our setup using dichroic B, and using three samples with three different concentrations of rhodamine 6G dissolved in ethanol: .2 μM , 2 μM , and 20 μM . We used exposure times of 5 seconds, 0.5 seconds, and 0.05 seconds so the number of counts would be roughly equal (around 20000 for all three measurements). We used rolling shutter mode and imaged the middle 500x500 pixels of the camera. The background signal of the ethanol was determined to be 607/451 for camera 1 / camera 2 for an exposure time of 5 seconds, and negligible for exposure times of 0.5 and 0.05 seconds (so equal to the fundamental background 103/103). We determined the G-value images for all three rhodamine samples, using the ethanol background values we found. We then calculated the average

G-factor over the middle 300x300 pixels of the chip (to make sure we don't take strange values near the edges into account). The average G-factors came out to be 1.2300, 1.2340, and 1.2334 for the $.2 \mu M$, $2 \mu M$, and $20 \mu M$ concentrations. This tells us that the G-factor is not dependent on the rhodamine concentration, and also suggests that the G-factor can be determined up to an accuracy of about 0.003. We shall refer to this as the fundamental uncertainty in G.

7.10 G-factor measurements with dichroic C

We measured the G-factor of our setup using dichroic C, and using the $5 \mu M$ BSA pre-treated rhodamine B sample described in section 4.2. We used an exposure time of 0.2 seconds, using the rolling shutter setting. We also measured the background using a BSA-treated sample containing no rhodamine, under the same conditions. All measurements were done using the middle 500x500 pixels of the chip. The BSA background averaged over the whole 500x500 pixel area was consistently 113/108 (camera 1/camera 2). We subtracted this background from the rhodamine measurements and calculated the G-factor image. This image can be seen in figure 10. We see that the G-factor varies over the image on the order of 0.1. Also note the black bars that result from image alignment close to the edge of the figure. The average G-factor over the middle 300x300 pixels was 1.2946. This is significantly higher than what we found for dichroic B. However the alignment of the setup was also different, and seeing as G varies by up to 0.1 over the image, it is not hard to imagine that a different alignment can give a very different G-factor image. Upon further inspection we found the variation in G on a pixel by pixel basis to be about 0.015 (by this we mean the standard deviation in G (not averaged) over a small area). Since we have a fundamental uncertainty of 0.003 (see previous section), and the standard deviation in an average is inversely proportional to the square root of the number of pixels averaged over, we see that the uncertainty in average G over any area larger than about 25 pixels is equal to the fundamental uncertainty.

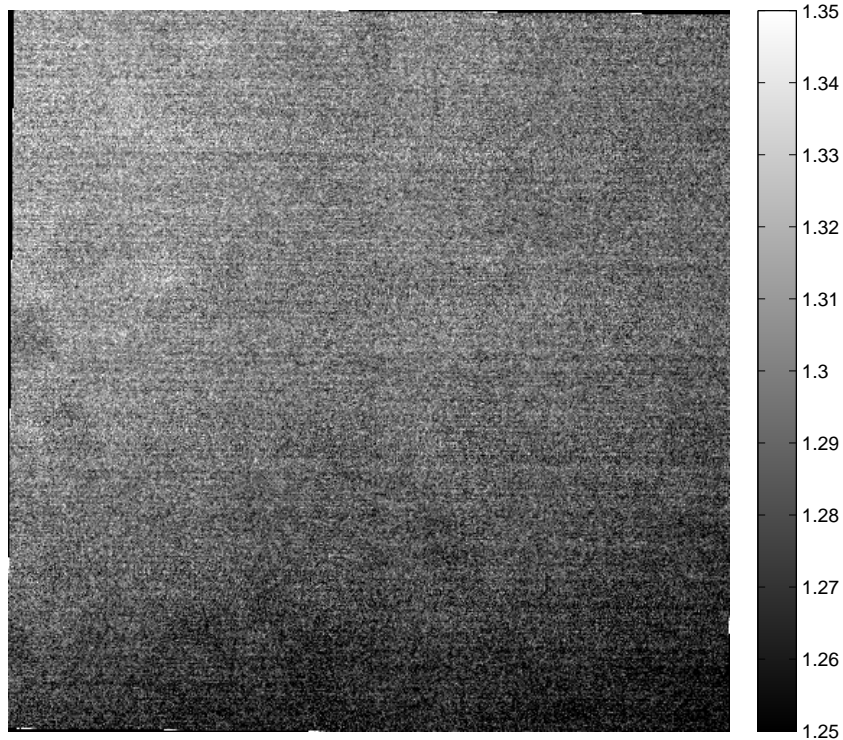


Figure 10: The G-factor image for dichroic C, measured using a $5 \mu M$ BSA pre-treated rhodamine B sample.

7.11 The anisotropy of mCherry in glycerol

We imaged a BSA-pre-treated $5\ \mu M$ solution of mCherry in glycerol, as described in section 4.3. We used an exposure time of 0.2 seconds and we used the rolling shutter mode to image the middle 500×500 pixels of each camera. We also measured the background caused by an identically prepared sample with no mCherry. This background was consistently about 110/105 (camera 1/camera 2). We subtracted this background before calculating the anisotropy image (see figure 11). We see that the anisotropy varies on the order of 0.01. The average anisotropy over the middle 300×300 pixels is 0.3223. Now, if mCherry in glycerol had a base anisotropy of 0.4, we would expect an anisotropy of about 0.375 because of the anisotropy lowering effect of the objective. Therefore, other depolarizing factors must be at play here. We calculated the effects of rotational diffusion on the anisotropy but this turned out to be negligible. Due to the relatively high concentration of the sample, the average distance between two mCherry molecules is about 70nm. this means that some of the mCherry molecules might be close enough to exhibit FRET, even without dimerization. When we actually calculated this effect it turned about to be negligible as well. Another possibility is that mCherry does show some dimerization despite its name, and that this causes FRET. If we assume that the dissociation constant is equal to that of GFP (so $k_D \approx 100\mu M$), then 8% of the mCherry molecules would be dimerized. This would lower the anisotropy by about 0.02. Therefore we measured the anisotropy of another mCherry sample with a much lower concentration ($0.5\ \mu M$). The average anisotropy for the middle 300×300 pixels now came out to be 0.3410. It seems that some FRET due to dimerization did occur. Since the dissociation constant for mCherry is at least $25\ \mu M$ [18], the anisotropy probably won't increase any further with lower concentrations of mCherry.

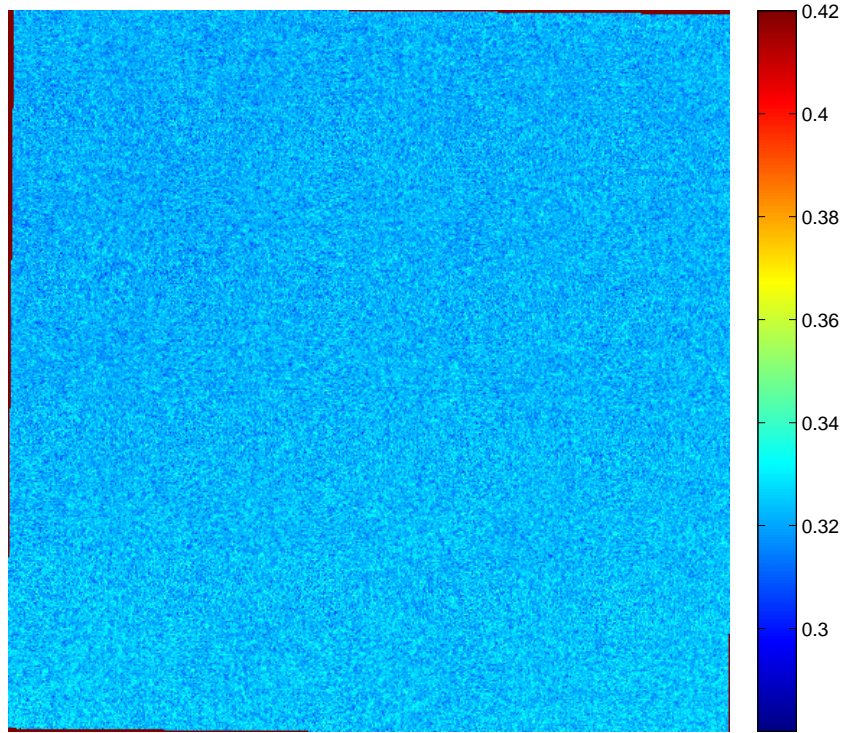


Figure 11: The anisotropy image of a $5\ \mu M$ solution of mCherry in glycerol.

7.12 Autofluorescence with dichroics A and C

We measured the autofluorescence of 20 unlabeled endothelial rat cells, using both dichroic A and C. The imaged cells were put in the same location on the camera every time (the middle 500x500 pixels), and the exposure time was 10 seconds, using the rolling imaging setting. The cells were very dim, so it was hard to make out features like the nucleus and the membrane. Therefore we just measured the average intensity over entire cells, using the free-hand tool in *ImageJ*. We found the average autofluorescence using dichroic A to be 395/246 (camera 1/camera 2), and using dichroic C to be 845/435. We calculated the standard deviation of the average intensities of the cells. This came out to be 49/16 for dichroic A and 62/22 for dichroic C. We also measured the internal intensity variation within cells. This seemed to be about 75/25 for dichroic A and 200/75 for dichroic C. Finally, we determined the background by measuring the average intensity around the cells. This was about 340/225 for dichroic A and 720/390 for dichroic C. Subtracting this background from the average autofluorescence intensities we find the true autofluorescence (actually caused by the presence of the cell) to be about 55/20 for dichroic A and 125/45 for dichroic C. We see that both the true autofluorescence and the total autofluorescence (including background) are about twice as high for dichroic C. However, since the excitation beam using dichroic C is about six times as intense, and the emission band filter of dichroic C is twice as wide, the autofluorescence of the cells is about 5 to 10 times as dim in the red part of the spectrum.

7.13 Re-evaluation of uncertainties

In this section, we will use our reference measurements and equation 38 to estimate the final anisotropy uncertainty for mCherry labeled cells, imaged with our setup. First of all, we can estimate how many counts we will get from the cells by looking at Nivard Kagie's measurements with GFP-transfected cells. Using the global imaging setting and an imaging time of ten seconds the GFP transfected cells yielded on the order of 5000 counts per pixel [1]. This would be equivalent to about 15000 counts using the rolling setting. If we assume that mCherry transfected cells will have the same label-concentration as the GFP transfected cells, we can therefore expect about 15000 counts using an imaging time of 0.2 seconds (because mCherry gives us 50 times as many counts in our setup). At this imaging time, the autofluorescence will be roughly equal to the fundamental background, and the variation in it will be negligible. The only non-systematic uncertainties that remain are therefore photon statistics and the uncertainty in the G-factor. Assuming parallel/perpendicular intensities of 15000/4500, a $\sqrt{\alpha}$ factor of 1.3, a G-factor of 1.3 and an uncertainty (single pixel) in the G-factor of 0.02 we get an uncertainty in the anisotropy of 0.010. This represents the anisotropy uncertainty in a single pixel. This also agrees with the anisotropy variation we saw in figure 11. When we are talking about the average anisotropy in a small area, the photon statistics uncertainty becomes negligible and we can assume the uncertainty in G to be equal to the fundamental uncertainty, 0.003. Using the same values as before we now get an uncertainty of about 0.0015. To be safe we'll estimate the final uncertainty in our anisotropy to be about 0.002. Please note that this is still a best case scenario and the uncertainty still heavily depends on the intensity we can get from mCherry labeled cells. If it turns out that we only get one tenth of the number of counts, the uncertainty in small-area averaged anisotropy goes to 0.01.

8 Conclusions

The most important conclusions we were able to draw from our measurements are:

- The autofluorescence of endothelial cells is about 5 to 10 times greater in the green part of the spectrum than in the red part. Using a red labeling protein therefore significantly reduces the anisotropy uncertainty caused by autofluorescence.
- Using a good fluorophore-dichroic combination is a crucial factor in getting the high intensities necessary for accurate anisotropy measurements.
- Using our setup we should be able to determine the anisotropy in a cell up to an accuracy of about 0.01 for single pixels, and 0.002 for small areas.

9 Discussion

In this section we discuss some of our results/assumptions.

9.0.1 Choosing wide-field over confocal

For our experiment we chose to use wide-field microscopy over confocal microscopy because it yields more light and the imaging time is much lower. However, since we discovered that mCherry in combination with dichroic C can give us very high intensities, we could consider using confocal microscopy as well. As every pixel needs to be imaged separately, our total imaging time will be proportional to the amount of pixels in our image. A cell can be captured in an area of about $100 \times 100 \approx 10000$ pixels, so making a confocal image with an intensity equal to our wide-field images would take an imaging time of $10000 \times 0.2 = 2000$ seconds. However, we can get away with lowering the imaging time per pixel by a factor of about ten while keeping reasonably accurate anisotropy. Using this the total confocal imaging time would be reduced to 200 seconds. Now if we imagine also using a more intense light source we can see that confocal anisotropy microscopy might be possible. Confocal anisotropy microscopy would give us depth resolution which would help in eliminating background (as in light from fluorophores which are not in the same horizontal plane), and could provide better contrast in our images (see also [2]).

9.0.2 Alignment using a different dichroic

In section 7.8 we concluded that using a different dichroic for alignment of the cameras doesn't matter since the three different green dichroics we used resulted in the same T-matrix. However, since the dichroics all had to be able to be used to image the beads, they all had similar emission band filters. Therefore the differences between the wavelengths of the final bead images are small. Since we have a number of elements in the emission path which are wavelength dependent, it could be that dichroic C actually does require separate alignment. Therefore, for future experiments we recommend using the same dichroic for both alignment and measurements.

9.0.3 mCherry measurements

When we determined the maximum anisotropy for our setup using solutions of mCherry, we found a higher anisotropy for a $0.5 \mu M$ solution than for a $5 \mu M$ solution. We therefore concluded that at $5 \mu M$ there must have been a FRET effect due to dimerization. We remarked that lowering the concentration further would probably not increase the anisotropy further, since [18] found indications that the dimerization constant of mCherry is at least $25 \mu M$. However, this was for mCherry in a live cell, not for mCherry in glycerol. It is quite possible that mCherry in glycerol has a lower k_D , so that using a concentration lower than $0.5 \mu M$ actually would increase the anisotropy. We therefore recommend carrying out anisotropy measurements with lower concentrations of mCherry in the future.

References

- [1] *Homo-FRET Detection by Fluorescence Polarization Anisotropy in Wide-field Microscopy*
N. Kagle, Utrecht University, 2013.
- [2] *Homo-FRET Imaging Enables Quantification of Protein Cluster Sizes with Subcellular Resolution*
A.N. Bader, E.G. Hofman, J. Voortman, P.M.P. van Bergen en Henegouwen, and H.C. Gerritsen, 2009.
- [3] *Principles of Fluorescence Spectroscopy (3rd edition)*
ISBN 0387312781
Joseph. R. Lakowicz, 2010.
- [4] *Theory and application of fluorescence homotransfer to melittin oligomerization.*
<http://www.ncbi.nlm.nih.gov/pubmed/8534828>
L.W. Runnels and S.F. Scarlata, State University of Stony Brook, New York, 1995.
- [5] *Electronic excitation energy transfer in condensed matter*
ISBN 0444863354
V.M. Agranovich and M.D. Galanin, 1982.
- [6] *Eurofins*
<http://www.eurofinsgenomics.eu/en/dna-rna-oligonucleotides/customised-dna-oligos/modified-dna-oligos/fluorescent-dyes.aspx>
- [7] *Oregon Medical Laser Center*
<http://omlc.ogi.edu/>
- [8] *UCI Optical Biology Core Facility*
<http://dbc.bio.uci.edu/OBCresources/fluorophores.pdf>
- [9] *A guide to choosing fluorescent proteins*
<http://www.tsienlab.ucsd.edu/Publications/Shaner%202005%20Nature%20Methods%20-%20Choosing%20fluorescent%20proteins.pdf>
Nathan C. Shaner and Paul A. Steinbach and Roger Y. Tsien, UC San Diego, 2005.
- [10] *Fluorescent proteins at a glance*
<http://jcs.biologists.org/content/124/2/157.full.pdf>
Gert-Jan Kremers, Sarah G. Gilbert, Paula J. Cranfill, Michael W. Davidson and David W. Piston, 2011.
- [11] *Diffusion of Green Fluorescent Protein in the Aqueous-Phase Lumen of Endoplasmic Reticulum*
Mark J. Dayel, Erik F. Y. Hom, and A. S. Verkman, 1999.
- [12] *Rotational diffusion of rhodamine 6G depends on structural features of water and polyvinyl pyrrolidone mixtures*
<http://scitation.aip.org/docserver/fulltext/aip/journal/jcp/100/1/1.466944.pdf?expires=1386767315&id=id&accname=freeContent&checksum=02E349652FA39635377C59E16DE52242>
DongSeob Ko, 1994.
- [13] *Photochromicity and Fluorescence Lifetimes of Green Fluorescent Protein*
George Striker, Vinod Subramaniam, Claus A. M. Seidel, and Andreas Volkmer, 1999.
- [14] *ISS*
<http://www.iss.com/>
- [15] *Fluorescent proteins for single-molecule fluorescence applications.*
<http://www.ncbi.nlm.nih.gov/pubmed/19343637>
B. Seefeldt, R. Kasper, T. Seidel, P. Tinnefeld, K.J. Dietz, M. Heilemann, and M. Sauer, 2008.

- [16] *Biological Role of Epidermal Growth Factor-Receptor Clustering*
A. B. Schreiber, T. A. Libermann, I. Lax, Y. Yarden, and J. Schlessinger, 1982.
- [17] *CARBOCYANINE DYE ORIENTATION IN RED CELL MEMBRANE STUDIED BY MICROSCOPIC FLUORESCENCE POLARIZATION*
<http://www.ncbi.nlm.nih.gov/pmc/articles/PMC1328570/pdf/biophysj00290-0210.pdf>
D. Axelrod, University of Michigan, 1979.
- [18] *Fluorescence Fluctuation Spectroscopy of mCherry in Living Cells*
<http://www.ncbi.nlm.nih.gov/pmc/articles/PMC2907682/>
B. Wu, Y. CHen, and J.D. Müller, 2009.
- [19] *Andor Neo sCMOS Hardware Guide*
© Andor Technology plc 2011.
- [20] *Förster Distances between Green Fluorescent Protein Pairs*
G.H. Patterson, D.W. Piston, and B.G. Barisas, 2000.
- [21] *Förster distances for FRET between mCherry and other Visible Fluorescent Proteins*
N. Akrap, T. Seidel, and B.G. Barisas, 2010.

10 *MATLAB* Scripts

```
function af
%AF Sets figure properties for anisotropy figures.
caxis([0.28,0.42]); colormap(jet); set(gcf,'Color',[1,1,1]); colorbar; truesize;
```

```
function [T] = alim(im1, im2, Tstart)
%ALIM Determines the transformation between the cameras.
im3=im2;
if (nargin>2)
im2=imwarp(im2, Tstart,'OutputView',imref2d(size(im1)));
end

optimizer = registration.optimizer.RegularStepGradientDescent;
optimizer.MaximumIterations=500;
metric = registration.metric.MattesMutualInformation;

T = imregtform(im2, im1, 'affine', optimizer, metric);

if (nargin>2)
T.T=Tstart.T*T.T;
end

figure;
imshowpair(im1,imwarp(im3,T,'OutputView',imref2d(size(im1))));
end
```

```
function [ani] = aniplus(im1, im2, G, T, roi, auto)
%ANIPLUS Advanced form of anis.m using roi-autofluorescences.
l=size(auto);
l=l(1);

im1 = double(im1);
im2 = double(imwarp(im2, T,'OutputView',imref2d(size(im1))));

ani=im1-im1;
for i=1:l
ani = ani+ roi{i}.*(((im1-auto{i,1})-G.*(im2-auto{i,2}))./((im1-auto{i,1})+2*G.*(im2-auto{i,2})));
end
ani(isnan(ani))=0;
ani(isinf(ani))=0;
end
```

```
function [ani] = anis(im1, im2, G, T,auto1,auto2)
%ANIS Calculate anisotropy from 2 images and autofluorescence.
if nargin<6, auto1=0; auto2=0; end
if nargin<4, T = affine2d(); end
```

```

if nargin<3, G = 1; end

im1 = double(im1)-auto1;
im2 = double(imwarp(im2, T, 'OutputView', imref2d(size(im1))))-auto2;

ani = (im1-G.*im2)./(im1+2.*G.*im2);
ani(isnan(ani))=0;
ani(isinf(ani))=0;
figure; imshow(ani); af;

```

```

function [ava] = avanis(a,roi)
%AVANIS Calculate average anisotropies in regions of interest.
s=size(roi);
imax=s(1);
jmax=s(2);

for i=1:imax
for j=1:jmax
ava{i,j}=mean(nonzeros(roi{i,j}.*a{i}));
end
end
end

```

```

function [G]=calg(im1, im2, T)
%CALG Calculate your G-factor from images and transform-matrix.

if nargin<3
T=affine2d();
end

im2=imwarp(im2, T, 'OutputView', imref2d(size(im1)));

G = double(im1)./double(im2);
G(isnan(G))=0;
G(isinf(G))=0;
G(G>1.45)=0;
figure; imshow(G); ggf;
end

```

```

function ggf
%GF Sets figure properties for G-factor figures.
caxis([1.00,1.40]); colormap(gray); set(gcf,'Color',[1,1,1]); colorbar; truesize;
end

```

```

function [x,a]=process(link,G,T,auto1,auto2)
%PROCESS Process images from a path without regions of interest.
if nargin<5, auto1=0; auto2=0; end

```



```

if nargin<3, T = affine2d(); end
if nargin<2, G = 1; end

```

```

i=1;
while exist(strcat(link,'CAM1\',num2str(i),'.tif'))==2 && exist(strcat(link,'CAM2\',num2str(i),'.tif'))==2
x{i,1}=imread(strcat(link,'CAM1\',num2str(i),'.tif'));
x{i,2}=imread(strcat(link,'CAM2\',num2str(i),'.tif'));
a{i}=anis(x{i,1},x{i,2},G,T,auto1,auto2);
i=i+1;
end

```

```

function [x,a,m,roi]=process2(link,G,T,auto)
%PROCESS2 Old pipeline process function (not used).
l=size(auto);
l=l(2);
i=1;
while exist(strcat(link,'CAM1\',num2str(i),'.tif'))==2
x{i,1}=imread(strcat(link,'CAM1\',num2str(i),'.tif'));
x{i,2}=imread(strcat(link,'CAM2\',num2str(i),'.tif'));
    for j=1:l
        m{i,j}=~logical(imread(strcat(link,'MASK\',num2str(i),'m',num2str(j),'.tif')));
    end
    for j=1:l-1
        roi{i,j}=m{i,j}&~m{i,j+1};
    end
    roi{i,l}=m{i,l};

a{i}=aniplus(x{i,1}, x{i,2}, G, T, roi(i,:), auto);
figure; imshow(a{i}); af;
i=i+1;
end
end

```

```

function [x,a]=process3(link, G, T, roi, auto)
%PROCESS3 Process images from a path with regions of interest.
l=size(auto);
l=l(1);
i=1;
while exist(strcat(link,'CAM1\',num2str(i),'.tif'))==2
x{i,1}=imread(strcat(link,'CAM1\',num2str(i),'.tif'));
x{i,2}=imread(strcat(link,'CAM2\',num2str(i),'.tif'));
a{i}=aniplus(x{i,1}, x{i,2}, G, T, roi(i,:), auto);
figure; imshow(a{i}); af;
i=i+1;
end
end

```

```

function [roi] = roifrommask(link,imnum,propnum,inverted)
%ROIFROMMASK Make a cell of regions of interest (logical) from tif-masks.

```

```

if(nargin)<4
inverted=0;
end

for i=1:imnum
    if inverted==0
        for j=1:propnum
            m{i,j}=logical(imread(strcat(link,num2str(i),'m',num2str(j),'.tif')));
        end
    end
    if inverted==1
        for j=1:propnum
            m{i,j}=~logical(imread(strcat(link,num2str(i),'m',num2str(j),'.tif')));
        end
    end
    for j=1:propnum-1
        roi{i,j}=m{i,j}&~m{i,j+1};
    end
    roi{i,propnum}=m{i,propnum};
end
end

```

```

function sav(x,place,name)
%SAV Save a cell of images (x) to a location and give them a name
s=size(x);
s=s(2);

for i=1:s
imwrite(uint16(x{i}),strcat(place,name,num2str(i),'.tif'));
end

```

```

function savanis(a,place,name)
%SAVANIS Save your anisotropy cell as data images and as figures.
s=size(a);
s=s(2);

for i=1:s
imwrite(uint16(1000*a{i}),strcat(place,name,num2str(i),'.tif'));
figure; imshow(a{i}); af; print('-depsc',strcat(place,'figure_',name,num2str(i))); close;
end

```